TECHNICAL NOTE

D-855

A STUDY OF LAMINAR COMPRESSIBLE VISCOUS PIPE FLOW

ACCELERATED BY AN AXIAL BODY FORCE, WITH

APPLICATION TO MAGNETOGASDYNAMICS

By E. Dale Martin

Ames Research Center
Moffett Field, Calif.

NATIONAL AERONAUTICS AND SPACE ADMINISTRATION

WASHINGTON   April 1961

D

NATIONAL AERONAUTICS AND SPACE ADMINISTRATION

TECHNICAL NOTE D-855

A STUDY OF LAMINAR COMPRESSIBLE VISCOUS PIPE FLOW

ACCELERATED BY AN AXIAL BODY FORCE, WITH

APPLICATION TO MAGNETOGASDYNAMICS

By E. Dale Martin

SUMMARY

A study is made of the steady laminar flow of a compressible viscous
fluid in a circular pipe when the fluid is accelerated by an axial body
force. The application of the theory to the magnetofluidmechanics of an
electrically conducting gas accelerated by electric and magnetic fields
is discussed. Constant viscosity, thermal conductivity, and electrical
conductivity are assumed. Fully developed flow velocity and temperature
profiles are shown, and detailed results of the accelerating flow develop-
ment, including velocity and pressure as functions of distance, are given
for the case where the axial body force is constant and for the case where
it is a linear function of velocity. From these results are determined
the pipe entry length and the pressure difference required.

INTRODUCTION

An electrically conducting fluid, such as a high-temperature ionized
gas, or a "seeded" gas, flowing in a channel or pipe can be accelerated
by an electric body force which is the result of application of mutually
perpendicular electric and magnetic fields at right angles to the direction
of flow. A study of the electromagnetic interaction with a plasma is of
interest because of the possibility that the velocity of gas flow in a
wind tunnel or in the exhaust of a rocket or a jet engine can be substan-
tially increased by such an electromagnetically induced force. This
concept is mentioned, for example, by von Kármán (ref. 1), and devices
which utilize it have been investigated and described by Patrick (ref. 2)
and Ghai (ref. 3) among others. Thrust augmentation by this method may
be particularly useful in interplanetary flight because the achievable
specific impulses are likely to be high.

The theoretical magnetofluidmechanic channel flow has been treated
by numerous investigators. In particular, viscous incompressible flow
and accelerating inviscid compressible flow have been studied extensively.
Resler and Sears (refs. 4 and 5) have discussed and analyzed in some
detail certain aspects of fully developed viscous incompressible flow

and accelerating inviscid compressible flow. The problem of determining
entry length for the incompressible viscous flow of liquid metals in
pipes entering a region of uniform transverse magnetic field has been
studied by Shercliff (refs. 6, 7, and 8). Shercliff solved an unsteady
flow problem for a "settling time" or time to reach the steady state
after a magnetic field is applied. He then converted the settling time
to an approximate steady-flow entry length by multiplying the settling
time by the mean velocity of flow in the pipe. He showed by experiments
that the correct order of magnitude for entry length had been estimated.
References 6 and 7 dealt with flow between infinite parallel planes and
flow in rectangular pipes in which only nonconducting walls were consid-
ered. In reference 8 flow in a circular pipe with conducting walls was
studied. For that case the problem was treated in two stages: In the
first stage thin boundary layers developed with a core of uniform velocity;
then, in the second stage, the core profile was changed by electromagnetic
forces to its final form, with the boundary-layer thickness remaining
unchanged. The field of magnetohydrodynamics has recently been reviewed
by Sears (ref. 9) and by Rossow (ref. 10).

A
3
9
6

The present study treats the steady laminar flow of a viscous fluid
accelerated by an axial body force in a circular pipe but differs from
the study by Shercliff (ref. 8) in that the flow is considered to be
compressible rather than incompressible. The fluid is considered to
have a uniform velocity profile as it enters the pipe and to accelerate
until it approaches the "fully developed flow" condition, in which the
flow is exactly parallel and where there is no further acceleration or
change in the velocity profile. (For a liquid flowing in a pipe the fully
developed laminar flow is the familiar Hagen-Poiseuille pipe flow,
discussed in reference 11. Some effects of compressibility, variable
properties, and body forces on fully developed laminar flows in two-
dimensional channels have been studied by Maslen (ref. 12).) It is shown
that, when fully developed flow of a compressible fluid is defined simply
as a nonaccelerating parallel flow (which definition applies also to incom-
pressible fully developed flow), the necessary conditions for such a flow
to exist are that the axial gradients of density, pressure, and temperature
be zero and that a body force be supplied to sustain the flow. When these
conditions are supplied, via proper heat transfer to the wall and, for
example, electromagnetic body forces, then the body forces and viscous
shear forces can become balanced and the flow will approach an asymptotic
state.

Solutions for the fully developed flow velocity and temperature
profiles are found both for the case where the axial body force is
constant and for the case where it is a linearly decreasing function of
velocity. The development of the velocity profiles in the accelerating
portion of the flow is treated approximately. It is shown how these
solutions can be applied to the study of the magnetogasdynamic pipe-flow
problem in which the fluid is a conductor of electricity and the body
force is induced by electric and magnetic fields.

SYMBOLS

a	radius of pipe
A	defined by equation (15)
A_n	Fourier coefficient
B_I	$\dfrac{J_y H_o}{\sigma u_o H_o^2}$ in case I (see eq. (9))
B_{II}	$\dfrac{E_y}{H_o u_o}$ in case II
B_n	Fourier coefficient defined by equation (A3)
c_1, c_2	constants of integrations
C	defined by equation (46)
c_p	specific heat at constant pressure
D_n	Fourier coefficient defined by equation (A6)
E	electric field
E_e	electric field due to external effects
E_i	electric field due to internal separation of charges
Ω	Joule heating energy (eq. (54))
$\bar{\Omega}$	$\dfrac{a^2}{\mu u_o^2}\, \Omega$
f	function of λ_n, defined by equation (A10)
F	axial body force per unit volume
$\vec{F}$	body force vector per unit volume
$\bar{F}$	$\dfrac{a^2}{\mu u_o}\, F$
g	function of λ_n, defined by equation (A11)
G	function of $\bar{x}$, used first in equation (40)
h	function of λ_n, defined by equation (A17)
$\vec{H}$	magnetic field vector

H_O applied magnetic field in the z direction

I_O, I_1 modified Bessel functions of the first kind of orders zero and one

J current density

J_O, J_1 Bessel functions of the first kind of orders zero and one

k thermal conductivity

K $\sqrt{\dfrac{\sigma H_O^2 a^2}{\mu}}$, Hartmann number

M_O inlet Mach number

m ρu

$\bar{m}$ $\dfrac{a}{\mu} m = N_O \bar{\rho}\bar{u}$

n index of eigenfunctions

N_O $\dfrac{\rho_O u_O a}{\mu}$, Reynolds number at pipe inlet, based on radius

p thermodynamic pressure

$\bar{p}$ $\dfrac{a}{\mu u_O} p$

Pr $\dfrac{\mu c_p}{k}$, Prandtl number

$\vec{q}$ velocity vector

r distance normal to pipe axis

$\bar{r}$ $\dfrac{r}{a}$

R gas constant

R_n function of $\bar{r}$; solution of equation (28)

S_1, S_2, S_3 defined by equations (A14), (A15), and (A20), respectively

T temperature

$\bar{T}$ $\dfrac{c_p T}{u_O^2}$

A
3
9
6

u	velocity in the x direction
$\bar{u}$	$\dfrac{u}{u_O}$
U	difference in dimensionless velocities, defined by equation (20)
v	dimensionless specific volume, $\dfrac{1}{\rho}$
v_r	radial velocity component
x	axial distance from the pipe inlet
$\bar{x}$	$\dfrac{x}{a}$
X_n	function of $\bar{x}$
y	vertical coordinate perpendicular to pipe axis
z	horizontal coordinate perpendicular to pipe axis
α	constant of integration (eq. (29))
β	constant in equation (A7)
γ	ratio of specific heats
ϵ_n	defined by equation (27) for case I; by (51) for case II
η	function of $\bar{r}$ defined by either equation (67) or (82)
θ	coordinate angle in the y-z plane
λ_n	eigenvalue
μ	fluid viscosity
ξ	function of $\bar{r}$, defined by equation (36)
$\bar{\xi}$	function of $\bar{r}$, defined by equation (A5)
ρ	mass density of fluid
$\bar{\rho}$	$\dfrac{\rho}{\rho_O}$
σ	electrical conductivity

Subscripts and Superscripts

$(\ )_o$ value at $x = o$, $r = o$

$(\ )_\infty$ value at large $\bar{x}$

$(\ )_I$ case I (J_y = constant)

$(\ )_{II}$ case II (E_y = constant)

$(\ )_w$ value at the wall ($\bar{r} = 1$)

$(\ )_y$ component in the y direction

$\overline{(\ )}$ dimensionless quantity, except where defined otherwise

$\vec{(\ )}$ vector

$(\ )'$ differentiation with respect to $\bar{r}$

$(\ )^*$ value when velocity has approached to within 1 percent of fully developed flow velocity on the center line

EQUATIONS OF MOTION

Definition of the Problem

The steady high-speed compressible flow of a continuum gas in a semi-infinite straight circular pipe is considered. The fluid enters the pipe with high velocity at $x = 0$ (see fig. 1) and each fluid element is thereafter acted on by an axial body force. The Reynolds number $\rho u a / \mu$ is assumed to be low enough that viscous forces are important and that the flow is laminar. A compressible fluid flowing through a pipe may or may not approach an asymptotic state. If conditions are such that the viscous shear, pressure forces, and body forces in the fluid can become balanced, then the flow approaches the fully developed condition. Only cases in which the flow does approach this condition will be studied here. The necessary conditions for fully developed flow to occur (as described in the Introduction) will be derived in a later section.

Hypotheses Used and Their Effects on the Governing Equations

In order to conveniently study the flow, the following hypotheses are made: (1) the r and θ components of velocity (fig. 1) are nearly zero; (2) the flow is axially symmetric; (3) only axial body forces act

on the fluid; and (4) the viscosity is constant. The equations which result from application of these hypotheses to the flow conservation equations must be treated as approximations.

The first hypothesis indicates that the flow is approximately parallel. Although this is exactly true only for the fully developed flow, it is taken as a reasonable assumption for the accelerating portion of a high velocity compressible gas flow in a straight pipe. The continuity equation for the compressible flow of gas is then

$$\frac{\partial}{\partial x} (\rho u) \approx 0 \tag{1}$$

It must be noted that this equation must be treated as an approximation to the actual continuity equation; only in the special case of nonaccelerating flow can it exactly describe the true physical flow. For equation (1) to be exactly true in the accelerating flow, very special conditions on the heat transfer through the fluid and to the walls would be required. However, as will be seen, the analysis is greatly simplified by use of equation (1), and indications of the accuracy of the results will be shown later. The approximate equation (1) shows that ρu can be a function only of r, not of x; that is,

$$\rho u \approx m(r) \tag{2}$$

The implication is that each cylindrical lamina of fluid, at a distance r from the center of the pipe, moves as in a one-dimensional flow with ρu constant, the motion in each lamina being affected by the viscous forces due to the shear stresses on the adjacent fluid laminae. Near the pipe axis the viscous forces are small and the velocity of the fluid particles is greatly increased by the body forces, whereas near the wall, the higher viscous forces have a greater retarding effect. The density must therefore be greater near the wall. This is analogous to a compressible boundary layer adjacent to a cold wall, in which the density is higher near the wall. It might be noted that, in compressible boundary-layer solutions, one must consider v_r because the flow downstream of a point depends on what occurred at the point, that is, on the magnitudes of both components of velocity. If v_r were neglected in a boundary-layer problem where the downstream flow is not known but depends on the flow development upstream, errors in the solution of the downstream flow would be compounded because of inexactness of the solution upstream from a point. However, in the present problem, precise knowledge of v_r is not necessary to prevent such a compounding of errors because the solution is forced to approach the known exact solution of the equations governing the downstream fully developed flow, as will be shown later.

The momentum equations which govern the motion reduce from the compressible Navier-Stokes equations in cylindrical coordinates to the following form:

$$\rho u \frac{\partial u}{\partial x} = F - \frac{\partial p}{\partial x} + \frac{4}{3} \mu \frac{\partial^2 u}{\partial x^2} + \frac{\mu}{r} \frac{\partial}{\partial r} \left(r \frac{\partial u}{\partial r} \right) \tag{3}$$

$$0 = - \frac{\partial p}{\partial r} + \frac{1}{3} \mu \frac{\partial^2 u}{\partial x \, \partial r} \tag{4}$$

where F is the axial body force per unit volume. If F is constant or a known function of any of the other variables, equations (1), (3), and (4) comprise a determinate set, and hence the velocity u can be found. Before proceeding to discussions of F and the solution of the equations, however, the term containing ρu in equation (3) requires further discussion. The result of the approximate equation (1) is the relationship in equation (2), which determines the product ρu if it is known at any x. One must keep in mind, however, that, in the equations for a compressible gas, the density is related to the temperature, pressure, and velocity through the energy equation and the equation of state, as well as the continuity equation and the momentum equations. (These relations are discussed in a later section.) If the gas flow is to become fully developed, the density will assume a certain profile governed by these equations. It is not to be expected that ρu will have exactly the same distribution profile at $x = \infty$, where the flow becomes fully developed, as it happens to have at $x = 0$. It is therefore evident that ρu is not strictly a function of r, but may also be a slowly varying function of x. These considerations, however, do not invalidate the use of equation (2) in finding the velocity and pressure from equations (3) and (4) in the regions where $\partial u / \partial x$ is not zero for the following reasons. The only instance where ρu occurs in the momentum equations is in the term $\rho u (\partial u / \partial x)$. This term, therefore, is approximated by $\rho_0 u_0 (\partial u / \partial x)$. At $x = 0$, the acceleration $\partial u / \partial x$ is large, but the term is exact because $\rho u \equiv \rho_0 u_0$. As x increases from zero, ρu remains nearly $\rho_0 u_0$ as $\partial u / \partial x$ decreases. As x approaches infinity, the actual ρu profile approaches $\rho_\infty u_\infty$, but $\partial u / \partial x$ approaches zero and the term becomes very small. Thus it is seen that the term $\rho u (\partial u / \partial x)$ is important near $x = 0$ where $\rho u \approx \rho_0 u_0$, but its exact value is not as important at larger values of x.

Body Forces and Electromagnetic Phenomena

In the application of the solution of equations (2), (3), and (4) to the magnetogasdynamic problem, F is the axial electric body force induced by electric and magnetic fields applied perpendicular to the

flow direction. If the magnetic permeability of the fluid is assumed to be the same as that of empty space, the electric body force per unit volume is

$$\vec{F} = \vec{J} \times \vec{H} \tag{5}$$

where $\vec{H}$ is the strength of the magnetic field and $\vec{J}$, the current density, is given by Ohm's law:

$$\vec{J} = \sigma(\vec{E} + \vec{q} \times \vec{H}) \tag{6}$$

Figure 2 indicates schematically the electric and magnetic fields. A uniform magnetic field, H_O, is applied in the z direction. An appropriate distribution of electrical potential is applied to the conducting walls of the pipe. The fields are considered to be applied starting at the pipe inlet, $x = 0$. The interaction of the electric and magnetic fields is governed by Maxwell's field equations. The fields are, in turn, coupled with the fluid velocity by Ohm's law. It will be assumed that the z component of $\vec{H}$ does not vary appreciably from the value H_O and that the magnitudes of the components induced in the x and y directions are small. These assumptions require that the magnetic Reynolds number $\sigma u_O a$ be low. This has been discussed by Rossow (ref. 10) and by Hains and Yoler (ref. 13) among many others. Equations (5) and (6) then give for the axial body force

$$F = \sigma H_O(E_y - uH_O) \tag{7}$$

The electric field $\vec{E}$ is due to the internal separation of charges (polarization) as well as to the effect of the charged boundaries. It may be helpful to look at equation (6) in the form

$$\vec{q} \times \vec{H} = \frac{1}{\sigma} \vec{J} - \vec{E}_e - \vec{E}_i \tag{8}$$

where $\vec{E}_e$ is the electric field due to external effects (charged boundaries) and $\vec{E}_i$ is due to separation of charges. Thus, from equation (8), it is seen that the induced emf, $\vec{q} \times \vec{H}$, has two effects: that of driving a current through the gas and that of separating charges (from discussion by Resler and Sears in ref. 4).

The problem at hand will now be considered from two points of view. In case I it will be hypothesized that the current density component J_y is constant (fig. 2(a)). (Note that the purpose of this hypothetical case is to give a simple form for the body force, and it will probably be difficult to achieve in the circular pipe flow. Resler and Sears in reference 4 have shown it to be nearly true for two-dimensional channel flow through crossed fields.) Then, for case I, the electric body force, from equation (7), becomes

$$F_I = \sigma H_O(E_y - uH_O) = \text{constant}$$

where σ is also assumed to be a scalar and to have a constant finite value, or

$$F_I = \left(\frac{\mu u_o}{a^2}\right) K^2 B_I$$

where

$$B_I = \frac{J_y H_o}{\sigma u_o H_o^2} = \left(\frac{E_y}{H_o u_o} - \frac{u}{u_o}\right) = constant$$

$$(9)$$

and where

$$K^2 = \frac{\sigma H_o^2 a^2}{\mu}$$

The symbol K is the Hartmann number (ref. 14), whose square is the product of the Reynolds number, the magnetic Reynolds number, and the magnetic pressure number. In this case E_y, the y component of the electric field, varies because u is a variable. Case II (fig. 2(b)) will be the situation where the configuration and design of the apparatus and the magnitudes of the fields are such that E_y can be assumed to be nearly constant. This can conceivably be true for large applied electric fields and for appropriate conducting properties and construction of the pipe wall. Thus, for case II, it is hypothesized that E_y is constant, and the electric body force per unit volume is a variable and has the form

$$F_{II} = \sigma H_o^2 \left(\frac{E_y}{H_o} - u\right) = \left(\frac{\mu u_o}{a^2}\right) K^2 \left(B_{II} - \frac{u}{u_o}\right)$$

where

$$B_{II} = \frac{E_y}{H_o u_o}$$

$$(10)$$

The Approximate Dimensionless Equations of Motion

Equations (2), (3), and (4) will now be studied for both case I and case II where the body force has the form given by equations (9) and (10), respectively. The parameters may be made dimensionless as follows:

$$\bar{u} = \frac{u}{u_o} \qquad \bar{p} = \frac{ap}{\mu u_o} \qquad N_o = \frac{\rho_o u_o a}{\mu}$$

$$\bar{x} = \frac{x}{a} \qquad \bar{\rho} = \frac{\rho}{\rho_o} \qquad \bar{m}(\bar{r}) = \frac{am}{\mu} = \frac{\rho u a}{\mu} = N_o \bar{\rho}\bar{u}$$

$$\bar{r} = \frac{r}{a} \qquad \bar{F} = \frac{a^2 F}{\mu u_o} \qquad K^2 = \frac{\sigma H_o^2 a^2}{\mu}$$

Then equations (3) and (4), using equation (2), become

$$\bar{m}(\bar{r})\,\frac{\partial \bar{u}}{\partial \bar{x}} = \bar{F} - \frac{\partial \bar{p}}{\partial \bar{x}} + \frac{4}{3}\,\frac{\partial^2 \bar{u}}{\partial \bar{x}^2} + \frac{1}{\bar{r}}\,\frac{\partial}{\partial \bar{r}}\left(\bar{r}\,\frac{\partial \bar{u}}{\partial \bar{r}}\right) \tag{11}$$

$$0 = -\frac{\partial \bar{p}}{\partial \bar{r}} + \frac{1}{3}\,\frac{\partial^2 \bar{u}}{\partial \bar{x}\,\partial \bar{r}} \tag{12}$$

where, for case I,

$$\bar{F} = \bar{F}_I = K^2 B_I \tag{13a}$$

and, for case II,

$$\bar{F} = \bar{F}_{II} = K^2(B_{II} - \bar{u}) \tag{13b}$$

A consequence of the foregoing hypotheses and assumptions is that the energy and momentum equations are not coupled, so they can be treated separately, and the momentum equations are linear after substitution of the approximation $\rho u(\partial u/\partial x) \approx \rho_0 u_0 (\partial u/\partial x)$.

SOLUTION OF THE EQUATIONS OF MOTION

Case I ($\bar{F} = K^2 B_I = $ Constant)

Fully developed flow.- As $\bar{x}$ approaches infinity the flow approaches the fully developed flow condition and $\partial \bar{u}/\partial \bar{x}$ approaches zero. If this condition is imposed on equations (11) and (12), and if the dimensionless velocity for fully developed flow is denoted as $\bar{u} = \bar{u}_\infty(\bar{r})$, the resulting differential equation for case I is

$$\frac{1}{\bar{r}}\,(\bar{r}\bar{u}_\infty{}')' = -4A \tag{14}$$

where $(\ )'$ indicates differentiation with respect to $\bar{r}$, and where:

$$A = \frac{1}{4}\left(K^2 B_I - \frac{d\bar{p}_\infty}{d\bar{x}}\right) \tag{15}$$

$$\bar{p} = \bar{p}_\infty(\bar{x}) \tag{16}$$

$$\frac{d\bar{p}_\infty}{d\bar{x}} = \text{constant} \tag{17}$$

Equation (16) results directly from equation (12), and equation (17) is easily deduced by observing that all other parts of equation (14) are functions only of $\bar{r}$. The boundary conditions are:

$$\bar{r} = 0 , \quad \bar{u}_\infty \text{ is finite} \tag{18a}$$

$$\bar{r} = 1 , \quad \bar{u}_\infty = 0 \tag{18b}$$

The solution of equation (14), with the boundary conditions (18a) and 18(b), is

$$\bar{u}_\infty(\bar{r}) = A(1 - \bar{r}^2) \tag{19}$$

where A is defined by equation (15).

Development of the flow from a uniform profile.- A new variable U may be defined by

$$U(\bar{x},\bar{r}) = \bar{u}_\infty(\bar{r}) - \bar{u}(\bar{x},\bar{r}) \tag{20}$$

where the function $\bar{u}_\infty(\bar{r})$ is the fully developed dimensionless velocity profile, and $\bar{u}(\bar{x},\bar{r})$ is the actual dimensionless velocity at a point in the pipe between the inlet, $\bar{x} = 0$, and a high value of $\bar{x}$ where the flow is considered to be fully developed. Substitution of equation (20) into equations (11) and (12), using (13a), gives

$$\bar{m} \frac{\partial U}{\partial \bar{x}} = -F_I + \frac{\partial \bar{p}}{\partial \bar{x}} + \frac{4}{3} \frac{\partial^2 U}{\partial \bar{x}^2} + \frac{1}{\bar{r}} \frac{\partial U}{\partial \bar{r}} + \frac{\partial^2 U}{\partial \bar{r}^2} - \left(\bar{u}_\infty{}'' + \frac{1}{\bar{r}} \bar{u}_\infty{}' \right) \tag{21}$$

$$\frac{\partial \bar{p}}{\partial \bar{r}} + \frac{1}{3} \frac{\partial^2 U}{\partial \bar{x} \partial \bar{r}} = 0 \tag{22}$$

If equation (21) is differentiated with respect to $\bar{r}$, equation (22) is differentiated with respect to $\bar{x}$, and the resulting equations are combined, the result is

$$\frac{\partial^3 U}{\partial \bar{r}^3} + \frac{1}{\bar{r}} \frac{\partial^2 U}{\partial \bar{r}^2} - \frac{1}{\bar{r}^2} \frac{\partial U}{\partial \bar{r}} + \frac{\partial^3 U}{\partial \bar{x}^2 \partial \bar{r}} - \frac{\partial}{\partial \bar{r}} \left(\bar{m} \frac{\partial U}{\partial \bar{x}} \right) = 0 \tag{23}$$

where use has been made of the fact that, from equation (14), $(\bar{u}_\infty{}'' + (1/\bar{r})\bar{u}_\infty{}')$ is a constant.

In the present problem, the velocity at the pipe inlet is uniform, that is, $\bar{u}(0,\bar{r}) = 1 \ (0 \leq \bar{r} < 1)$. The density profile at the inlet is also considered to be uniform, so that $\bar{\rho}(0,\bar{r}) = 1$ and $\bar{m}(\bar{r}) \approx \bar{m}_0(\bar{r}) = N_0$, a constant, $(0 \leq \bar{r} < 1)$. The boundary conditions on $\bar{u}$ are thus:

$$\left.\begin{array}{lll} \overline{x} = 0 \ , & \overline{u} = 1 \ , & (0 \leq \overline{r} < 1) \\[2mm] \overline{x} = \infty \ , & \overline{u} = \overline{u}_\infty(\overline{r}) \\[2mm] \overline{r} = 0 \ , & \overline{u} \ \text{is finite} \\[2mm] \overline{r} = 1 \ , & \overline{u} = 0 \end{array}\right\} \quad (24)$$

The corresponding conditions on U are, therefore:

$$\overline{x} = 0 \ , \qquad U = \overline{u}_\infty(\overline{r}) - 1 \ , \qquad (0 \leq \overline{r} < 1) \tag{25a}$$

$$\overline{x} = \infty \ , \qquad U = 0 \tag{25b}$$

$$\overline{r} = 0 \ , \qquad U \ \text{is finite} \tag{25c}$$

$$\overline{r} = 1 \ , \qquad U = 0 \tag{25d}$$

Particular solutions to equation (23) may be assumed to have the product form, $X(\overline{x})R(\overline{r})$. The complete solution is the linear combination of all possible solutions. Substitution of the product XR into equation (23) then gives the result

$$U(\overline{x},\overline{r}) = \sum_{n=1}^{\infty} A_n e^{\epsilon_n \overline{x}} R_n(\overline{r}) \tag{26}$$

where

$$\epsilon_n = \frac{1}{2} \, N_0 \left[1 - \sqrt{1 + \left(\frac{2\lambda_n}{N_0}\right)^2} \, \right] \tag{27}$$

and where λ_n^2 is the separation constant. (The positive sign on the radical has been eliminated by the boundary condition (25b).) The functions R_n are the solutions of

$$R''' + \left(\frac{1}{\overline{r}} \, R'\right)' + \lambda_n^2 R' = 0 \tag{28}$$

or

$$R'' + \frac{1}{\overline{r}} \, R' + \lambda_n^2 R = \alpha \tag{29}$$

where α is a constant of integration. The eigenvalues, λ_n, are to be determined. The boundary conditions on R are obtained from equation (26) with conditions (25c) and (25d). Thus

14

$$U(\overline{x},1) = \sum_{n=1}^{\infty} A_n e^{\epsilon_n \overline{x}} R_n(1) = 0$$

and

$$U(\overline{x},0) = \sum_{n=1}^{\infty} A_n e^{\epsilon_n \overline{x}} R_n(0) \quad \text{is finite}$$

Since both these statements must be true for all values of $\overline{x}$, it must be true that

$$R_n(1) = 0 \tag{30a}$$

and that

$$R_n(0) \quad \text{be finite} \tag{30b}$$

The solution to equation (29) is

$$R_n = c_1 J_0(\lambda_n \overline{r}) + c_2 Y_0(\lambda_n \overline{r}) + \frac{\alpha}{\lambda_n^2} \tag{31}$$

where J_0 and Y_0 are Bessel functions of the first and second kinds of order zero, and c_1 and c_2 are arbitrary constants.

Equation (31) involves three constants of integration, but only two direct conditions on $R_n(\overline{r})$ and its derivatives are available for the evaluation of the constants. These conditions, equations (30a) and (30b), will be used to evaluate c_1 and c_2. The remaining constant, α, will then be chosen so that other conditions of the problem are satisfied. This can be done indirectly by considering all possible values for α and determining the applicability of the results for each choice. The two classes of possible values for α that will be considered are: (1) $\alpha = 0$ and (2) $\alpha \neq 0$.

Consider first the possible case $\alpha = 0$. Application of conditions (30a) and (30b), along with the condition $\alpha = 0$, to equation (31) gives the results:

$$c_2 = 0 \tag{32}$$

and

$$J_0(\lambda_n) = 0 \tag{33}$$

Equation (26) may then be written

$$U(\overline{x}, \overline{r}) = \sum_{n=1}^{\infty} A_n e^{\epsilon_n \overline{x}} J_0(\lambda_n \overline{r}) \tag{34}$$

where the eigenvalues, λ_n, are the roots of equation (33).

Application of boundary condition (25a) to equation (34) leads to the result

$$\xi(\overline{r}) = \sum_{n=1}^{\infty} A_n J_0(\lambda_n \overline{r}) \tag{35}$$

where

$$\xi(\overline{r}) = \overline{u}_\infty(\overline{r}) - 1 , \qquad (0 \leq \overline{r} < 1) \tag{36}$$

The functions $J_0(\lambda_n \overline{r})$ are orthogonal with respect to $\overline{r}$ (cf. ref. 15). Therefore equation (35) represents the expansion of the function $\xi(\overline{r})$ in a series of orthogonal eigenfunctions (see again ref. 15), and A_n may be determined by the conventional method. Thus

$$A_n = \frac{\int_0^1 \xi(\overline{r}) J_0(\lambda_n \overline{r}) \overline{r} \, d\overline{r}}{\int_0^1 [J_0(\lambda_n \overline{r})]^2 \overline{r} \, d\overline{r}} \tag{37}$$

Using equations (19), (36), and (37), one obtains

$$A_n = \frac{2(4A/\lambda_n^2 - 1)}{\lambda_n J_1(\lambda_n)} \tag{38}$$

Thus the constant c_1 has been determined indirectly. It has been absorbed in A_n, which is determined by equations (33) and (38).

The dimensionless velocity $\overline{u}(\overline{x}, \overline{r})$ is now completely determined, for the constant α equal to zero, from equations (19), (20), and (34), along with equations (15), (27), (33), and (38).

One must consider now the possibility that α has a value other than zero. It will simply be noted here that it is shown in the appendix that the solutions obtained by letting α have any value other than zero are not possible. It is therefore established that

$$\alpha \equiv 0 \tag{39}$$

The pressure may now be found as follows: Integration of equation (22) gives

$$\overline{p} = -\frac{1}{3} \frac{\partial U}{\partial \overline{x}} + G(\overline{x}) \tag{40}$$

where $G(\overline{x})$ is to be determined. Then, if equation (40) is differentiated with respect to $\overline{x}$ and substituted into equation (21), and use is made of equations (14), (15), (26), (27), and (29), the following result is obtained:

$$G'(\overline{x}) = \frac{d\overline{p}_\infty}{d\overline{x}} \tag{41}$$

Integration of equation (41) and its substitution, along with equation (34), into equation (40) gives an expression which determines the pressure at any point to within a constant of integration. It would seem desirable, then, to find the constant of integration using the condition that, at $\overline{x} = 0$ and $\overline{r} = 0$, $\overline{p} = \overline{p}_0$. The following expression would result:

$$\overline{p} - \overline{p}_0 = \sum_{n=1}^{\infty} \frac{1}{3} A_n \epsilon_n \left[1 - e^{\epsilon_n \overline{x}} J_0(\lambda_n \overline{r}) \right] + \overline{x} \left(\frac{d\overline{p}_\infty}{d\overline{x}} \right) \tag{42}$$

Consider the case where $d\overline{p}_\infty/d\overline{x} = 0$ (this will later be shown to be the only possible case in fully developed flow). Equation (42), with the condition $\overline{x} \to \infty$, $\overline{p} \to \overline{p}_\infty$, then gives

$$\overline{p}_0 - \overline{p}_\infty = - \sum_{n=1}^{\infty} \frac{1}{3} A_n \epsilon_n \tag{43}$$

However, it is found that the above two equations are not convergent. But if the local pressure is related to the pressure at $\overline{x} = \infty$, for example, by adding equations (42) and (43), a result is obtained which converges for all $\overline{x}$ except $\overline{x} = 0$, because of the presence of the exponential term:

$$\overline{p} - \overline{p}_\infty = \sum_{n=1}^{\infty} - \frac{1}{3} A_n \epsilon_n e^{\epsilon_n \overline{x}} J_0(\lambda_n \overline{r}) \tag{44}$$

The pressure difference, $(\overline{p}_0 - \overline{p}_\infty)$, can then be found by calculating $(\overline{p} - \overline{p}_\infty)$ from equation (44) for small values of $\overline{x}$ and observing the limit approached as $\overline{x}$ approaches zero.

$$\text{Case II } [\overline{F} = K^2(B_{II} - \overline{u})]$$

Fully developed flow.- For this case, equations (11), (12), and (13b) result in

$$\overline{u}_\infty'' + \left(\frac{1}{\overline{r}}\right)\overline{u}_\infty' - K^2\overline{u}_\infty = -K^2 C \tag{45}$$

where

$$C = B_{II} - \frac{1}{K^2}\frac{d\overline{p}_\infty}{d\overline{x}} \tag{46}$$

$$\overline{p}_\infty = \overline{p}_\infty(\overline{x}) \; ; \qquad \frac{d\overline{p}_\infty}{d\overline{x}} = \text{constant} \tag{47}$$

With the boundary conditions (18a) and (18b), the solution to the fully developed flow equation, (45), is

$$\overline{u}_\infty(\overline{r}) = C\left[1 - \frac{I_0(K\overline{r})}{I_0(K)}\right] \tag{48}$$

where I_0 is the modified Bessel function of the first kind of order zero.

Development of the flow from a uniform profile.- As in case I, a new variable $U(\overline{x},\overline{r})$ is defined by equation (20). For this case $\overline{u}_\infty(\overline{r})$ is given by equation (48). Then, by an exactly analogous procedure as before, equations (11), (12), and (13b) give the partial differential equation:

$$\frac{\partial^3 U}{\partial\overline{r}^3} + \frac{1}{\overline{r}}\frac{\partial^2 U}{\partial\overline{r}^2} - \frac{1}{\overline{r}^2}\frac{\partial U}{\partial\overline{r}} - K^2\frac{\partial U}{\partial\overline{r}} + \frac{\partial^3 U}{\partial\overline{x}^2\partial\overline{r}} - \frac{\partial}{\partial\overline{r}}\left(\overline{m}\frac{\partial U}{\partial\overline{x}}\right) = 0 \tag{49}$$

As in case I, the velocity and density profiles at the pipe inlet are uniform so that

$$\overline{u}(0,\overline{r}) = 1 \; , \qquad (0 \leq \overline{r} < 1)$$

and

$$\overline{m}(\overline{r}) = N_0 \; , \qquad \text{a constant, } (0 \leq \overline{r} < 1)$$

The boundary conditions are then identical to equations (24) and (25). The solution to equation (49) is found by the same procedure as used in case I to be

18

$$U = \sum_{n=1}^{\infty} A_n e^{\epsilon_n \overline{x}} R_n(\overline{r})$$ (50)

where ϵ_n is now given by

$$\epsilon_n = \frac{1}{2} N_0 \left[1 - \sqrt{1 + \left(\frac{2}{N_0}\right)^2 (K^2 + \lambda_n{}^2)} \right]$$ (51)

and the functions R_n are the solutions of an equation identical to equation (29). The equations in the subsequent development are the same as equations (30) through (37). Equation (48) is then used along with equations (36) and (37) to obtain

$$A_n = \frac{2}{\lambda_n J_1(\lambda_n)} \left(\frac{CK^2}{\lambda_n{}^2 + K^2} - 1 \right)$$ (52)

In the development of equation (52), the integral $\int_0^1 I_0(K\overline{r}) J_0(\lambda_n \overline{r}) \overline{r} \, d\overline{r}$, which is similar to the Lommel integrals, was encountered. Its integration was handled in a manner following that used by McLachlan in reference 16 (pp. 94-95).

The dimensionless velocity $\overline{u}(\overline{x}, \overline{r})$ is thus determined for case II by equations (20), (34), and (48), along with equations (33), (46), (51), and (52). The impossibility of α having any value other than zero is shown in the appendix.

Following the same procedure used for case I, the pressure is found to be determined by an equation identical to equation (44), where A_n and ϵ_n, of course, correspond to case II.

ENERGY CONSIDERATIONS

Equations of State and Energy in Fully Developed Flow

Fully developed flow is considered to be a parallel flow in which the velocity profile does not change with streamwise distance. Maslen, in his study of fully developed gas flow in reference 12, states that, for a gas, none of the properties must be allowed to vary with axial distance. He obtains the result, then, that the velocity is only in the

x direction; that is, the flow is parallel. However, in the present study fully developed flow is defined exclusively in terms of velocity: $\vec{q} \equiv \vec{i}u$ where $\partial u/\partial x = 0$, and where $\vec{i}$ is the unit vector in the x direction. The author prefers to use this "nonaccelerating parallel flow" definition of fully developed flow, rather than a statement that nothing depends on x, in order to keep the defining statement identical to that used for incompressible fully developed flow, in which flow properties can vary with x. (Note that incompressible fully developed flow need not be defined to be parallel because it will be parallel if $\partial u/\partial x = 0$ to satisfy conservation of mass.) With this definition the result will be obtained that the flow properties cannot vary with x in fully developed laminar compressible viscous pipe flow.

In magneto-fluid dynamics the Joule heating term must be included in the energy balance on a fluid particle. The energy equation to be used is derived from a classical macroscopic point of view. The fluid is treated as a single-component system, and therefore no consideration of electrons, ions, or neutral particles is introduced (ref. 17). If the definition of fully developed flow ($\vec{q} \equiv \vec{i}u$ and $\partial u/\partial x = 0$), which leads to $u = u_\infty(r)$ and $v_r \equiv 0$ is used along with the results of the momentum and continuity considerations, $p = p_\infty(x)$ (i.e., p is at most a function only of x) and $dp_\infty/dx = $ constant, then the energy equation in fully developed laminar compressible viscous pipe flow of a conducting fluid (assuming k, μ, and c_p to be constant) is

$$\rho u c_p \frac{\partial T}{\partial x} = u \frac{dp_\infty}{dx} + k \left(\frac{\partial^2 T}{\partial r^2} + \frac{1}{r} \frac{\partial T}{\partial r} + \frac{\partial^2 T}{\partial x^2} \right) + \mu \left(\frac{du}{dr} \right)^2 + \Omega \qquad (53)$$

where $u = u_\infty(r)$ and where Ω is the Joule heating term:

$$\Omega = \frac{J^2}{\sigma} \qquad (54)$$

The equation of state is

$$p = \rho RT = \frac{\gamma - 1}{\gamma} \rho c_p T \qquad (55)$$

Because large temperature differences can exist in the flow in some cases, the fluid properties may vary considerably. The properties k, μ, c_p, and σ have been assumed to be constant in order to conveniently study the flow. The gas constant R is assumed constant, which implies that the number of particles per unit mass does not vary. Ohm's law, relating the electric field to the magnetic field and velocity (assuming $H_2 = H_0$), is

$$J_y = \sigma(E_y - uH_0) \qquad (56)$$

The parameters may be made dimensionless as before, with the additional parameters:

$$\overline{T} = \frac{c_p T}{u_o^2} , \qquad Pr = \frac{\mu c_p}{k} , \qquad \overline{\Omega} = \frac{a^2}{\mu u_o^2} \Omega$$

Equations (53) and (55) then reduce to:

$$N_o \overline{\rho}_\infty \overline{u}_\infty \frac{\partial \overline{T}}{\partial \overline{x}} = \overline{u}_\infty \frac{d\overline{p}_\infty}{d\overline{x}} + \frac{1}{Pr} \left(\frac{\partial^2 \overline{T}}{\partial \overline{x}^2} + \frac{1}{\overline{r}} \frac{\partial \overline{T}}{\partial \overline{r}} + \frac{\partial^2 \overline{T}}{\partial \overline{r}^2} \right) + \left(\frac{d\overline{u}_\infty}{d\overline{r}} \right)^2 + \overline{\Omega} \qquad (57)$$

and

$$\overline{p}_\infty(\overline{x}) = N_o \left(\frac{\gamma - 1}{\gamma} \right) \overline{\rho}_\infty \overline{T} \qquad (58)$$

where

$$\overline{\Omega} = K^2 \left(\frac{E_y}{H_o u_o} - \overline{u}_\infty \right)^2 \qquad (59)$$

Two cases have been considered in previous sections where it has been hypothesized that only axial body forces exist. The current density J is assumed to be only J_y, and σ is assumed constant. In the first case, J_y is considered to be a constant. Thus, for case I,

$$\overline{\Omega} = \overline{\Omega}_I = \text{constant} \qquad (60)$$

In case II, E_y is hypothesized to be constant. In that case, then

$$\overline{\Omega} = \overline{\Omega}_{II} = K^2 (B_{II} - \overline{u}_\infty)^2 \qquad (61)$$

where $B_{II} = E_y/H_o u_o$. Also considered here will be case III, conventional gas pipe flow, that is, the case where $\sigma = 0$ or $K^2 = 0$, with the result here that $\overline{\Omega} = 0$.

Temperature and Density in Fully Developed Flow
Corresponding to Case I

For case I, discussed above, combination of equations (57), (58), and (60) and use of the fact that $(\overline{\rho}_\infty \overline{u}_\infty)$ is a function only of $\overline{r}$ give

$$\frac{1}{\gamma - 1} \, \overline{u}_\infty \, \frac{d\overline{p}_\infty}{d\overline{x}} = \frac{\gamma}{\gamma - 1} \, \frac{\overline{p}_\infty(\overline{x})}{Pr \, N_O} \left(\frac{1}{\overline{r}} \, v_\infty{}' + v_\infty{}'' \right) + (\overline{u}_\infty{}')^2 + \overline{\Omega}_I \qquad (62)$$

where $\overline{\Omega}_I$ is a constant and

$$v_\infty(\overline{r}) = \frac{1}{\overline{\rho}_\infty(\overline{r})} \qquad (63)$$

There are only two possible ways in which equation (62) can be satisfied. It is known from the momentum equations that $d\overline{p}_\infty/d\overline{x}$ is a constant. Therefore, the only function of $\overline{x}$ in the equations is $\overline{p}_\infty(\overline{x})$. It is therefore concluded that either $\overline{p}_\infty$ is a constant or that

$$\frac{1}{Pr \, N_O} \left(\frac{1}{\overline{r}} \, v_\infty{}' + v_\infty{}'' \right) = 0$$

If the latter choice is considered, equation (62) becomes

$$(\overline{u}_\infty{}')^2 - \left(\frac{1}{\gamma - 1} \right) \frac{d\overline{p}_\infty}{d\overline{x}} \, \overline{u}_\infty + \overline{\Omega}_I = 0$$

It can be seen immediately that this equation is not compatible with the momentum equation. Its integration, in fact, yields an impossible result. Therefore this case is not possible, and it must then be true that $\overline{p}_\infty$ is a constant. The equation of state, (58), may then be rewritten, with $\overline{p}_\infty$ = constant,

$$\overline{T} = \frac{\gamma}{\gamma - 1} \, \frac{\overline{p}_\infty}{N_O \overline{\rho}_\infty(\overline{r})} \qquad (64)$$

to show that $\overline{T}$ can be a function only of $\overline{r}$, not of $\overline{x}$, that is,

$$\overline{T} = \overline{T}_\infty(\overline{r}) \qquad (65)$$

Therefore $\overline{T}_{\infty_W}$ is required to be constant.

The density and temperature profiles in fully developed flow may now be found from equation (62) as follows:

$$v_\infty{}'' + \frac{1}{\overline{r}} \, v_\infty{}' = \eta_I(\overline{r}) \qquad (66)$$

where

$$\eta_I(\bar{r}) = \left(\frac{1 - \gamma}{\gamma}\right) \frac{Pr\ N_O}{\bar{p}_\infty} \left[(\bar{u}_\infty')^2 + \bar{\Omega}_I\right] \qquad (67)$$

Using the result for $\bar{u}_\infty$ for case I from the momentum equation:

$$\bar{u}_\infty = \frac{1}{4} K^2 B_I(1 - \bar{r}^2) \qquad (68)$$

and the fact that

$$\bar{\Omega}_I = K^2 \left(\frac{E_y}{H_O u_O} - \bar{u}\right)^2 = K^2 B_I{}^2 \qquad (69)$$

equation (67) becomes

$$\eta_I = \left(\frac{1 - \gamma}{\gamma}\right) \left(\frac{Pr\ N_O}{\bar{p}_\infty}\right) K^4 B_I{}^2 \left(\frac{1}{4}\ \bar{r}^2 + \frac{1}{K^2}\right) \qquad (70)$$

Equation (66) may then be integrated, using the conditions

$$v_\infty(0) \quad \text{is finite} \qquad (71)$$

$$v_\infty(1) = N_O \left(\frac{\gamma - 1}{\gamma}\right) \frac{\bar{T}_{\infty_W}}{\bar{p}_\infty} \qquad (72)$$

(where eq. (72) is found from the equation of state, (64)) to give the fully developed flow density distribution:

$$\frac{1}{\bar{\rho}_\infty} = \frac{\gamma - 1}{\gamma} \frac{N_O}{\bar{p}_\infty} \left[\bar{T}_{\infty_W} + \frac{1}{4}\ Pr\ K^4 B_I{}^2 \left(\frac{1 - \bar{r}^4}{16} + \frac{1 - \bar{r}^2}{K^2}\right)\right] \qquad (73)$$

Equation (71) may then be combined with equation (64) to give a relation for the temperature profile in the fully developed flow:

$$\frac{\bar{T}_\infty - \bar{T}_{\infty_W}}{Pr} = \frac{1}{4} K^4 B_I{}^2 \left(\frac{1 - \bar{r}^4}{16} + \frac{1 - \bar{r}^2}{K^2}\right) \qquad (74)$$

Another variable of interest, the dimensionless mass-flow distribution, which was discussed earlier and which will be of use in a later section, is

$$\overline{m}_\infty(\overline{r}) = N_O \overline{\rho}_\infty \overline{u}_\infty = \frac{\left(\dfrac{\gamma}{\gamma - 1} \dfrac{\overline{p}_\infty}{Pr \, K^2 B_I}\right)\left(1 - \overline{r}^2\right)}{\dfrac{4\overline{T}_{\infty w}}{Pr(K^2 B_I)^2} + \dfrac{1}{16}\left(1 - \overline{r}^4\right) + \dfrac{1}{K^2}\left(1 - \overline{r}^2\right)} \tag{75}$$

Temperature and Density in Fully Developed Flow Corresponding to Case II

For case II, equations (57), (58), and (61) result in

$$\frac{1}{\gamma - 1} \overline{u}_\infty \frac{d\overline{p}_\infty}{d\overline{x}} = \frac{\gamma}{\gamma - 1} \frac{\overline{p}_\infty(\overline{x})}{Pr \, N_O}\left(\frac{1}{\overline{r}} v_\infty' + v_\infty''\right) + (\overline{u}_\infty')^2 + K^2(B_{II} - \overline{u}_\infty)^2 \tag{76}$$

From the momentum equations, $d\overline{p}_\infty/d\overline{x}$ is a constant. Therefore the only possible function of $\overline{x}$ in equation (76) is $\overline{p}_\infty(\overline{x})$. It again is concluded that either $\overline{p}_\infty(\overline{x})$ is a constant or $(1/Pr \, N_O)[(1/r)v_\infty' + v_\infty''] = 0$. The latter choice implies no radial heat transfer; that is, either $k = 0$ or $T \neq T(\overline{r})$. With this consideration, equation (76) becomes

$$(\overline{u}_\infty')^2 + K^2(B_{II} - \overline{u}_\infty)^2 - \frac{1}{\gamma - 1}\left(\frac{d\overline{p}_\infty}{d\overline{x}}\right)\overline{u}_\infty = 0 \tag{77}$$

But the solution for the fully developed flow velocity found from the momentum equation is

$$\overline{u}_\infty = C\left[1 - \frac{I_O(K\overline{r})}{I_O(K)}\right] \tag{48}$$

where

$$C = B_{II} - \frac{1}{K^2}\frac{d\overline{p}_\infty}{d\overline{x}} \tag{46}$$

For finite Hartmann number, equation (77) is contradictory to this solution (eq. (48)). However, let us consider for a moment the condition that Hartmann number approach infinity. Noting that

$$\frac{d\overline{p}_\infty}{d\overline{x}} = \frac{K^2}{\sigma u_O H_O{}^2}\frac{dp_\infty}{dx} \tag{78}$$

and that $\bar{u}_\infty$ and $\bar{u}_\infty{}'$ approach C and zero, respectively, in $(0 \leq \bar{r} < 1)$ as K approaches infinity, it is seen that equations (77) and (48) are then compatible in the region $(0 \leq \bar{r} < 1)$ if

$$\frac{dp}{dx} = \frac{\sigma E_y H_O}{\gamma} \tag{79}$$

so that

$$\bar{u}_\infty = \frac{\gamma - 1}{\gamma} B_{II} \ , \qquad \begin{cases} (0 \leq \bar{r} < 1) \\ K \to \infty \end{cases} \tag{80}$$

Because ρ cannot change in the x direction, equation (79) implies also that the temperature have a constant positive gradient in the x direction. This solution is not valid at the wall, that is, in the boundary layer, but it may be used in comparing the results of the present study with inviscid solutions in the case of no heat transfer. The flow described by equations (79) and (80) cannot, of course, be considered to be a fully developed _viscous_ flow because it requires that $\mu = 0$.

For case II, as for case I, therefore, the condition for fully developed compressible flow with nonzero viscosity is that $\bar{p}_\infty$ be a constant and that $d\bar{p}_\infty/d\bar{x} = 0$. It is then also required that $\bar{T} = \bar{T}_\infty(\bar{r})$ and thus that $\bar{T}_{\infty_W}$ be a constant. For the purpose of finding the density and temperature profiles, equation (76) may be written

$$v_\infty{}'' + \frac{1}{\bar{r}} v_\infty{}' = \eta_{II}(\bar{r}) \tag{81}$$

where

$$\eta_{II} = \left(\frac{1 - \gamma}{\gamma} \right) \frac{Pr \ N_O}{\bar{p}_\infty} [(\bar{u}_\infty{}')^2 + K^2(B_{II} - \bar{u}_\infty)^2] \tag{82}$$

and where, from equation (48),

$$\bar{u}_\infty = B_{II} \left[1 - \frac{I_O(K\bar{r})}{I_O(K)} \right] \tag{83}$$

After substitution of equation (83) and the relation

$$\bar{u}_\infty{}' = -B_{II}K \ \frac{I_1(K\bar{r})}{I_O(K)}$$

equation (82) becomes

$$\eta_{II}(\bar{r}) = \left(\frac{1-\gamma}{\gamma}\right) \frac{Pr\ N_O}{\bar{p}_\infty} \left[\frac{B_{II}K}{I_O(K)}\right]^2 [I_1^2(K\bar{r}) + I_O^2(K\bar{r})] \tag{84}$$

Equation (81) may then be integrated, using conditions identical to equations (71) and (72), to give

$$\frac{1}{\bar{\rho}_\infty} = \frac{\gamma-1}{\gamma} \frac{N_O}{\bar{p}_\infty} \left\{ \bar{T}_{\infty_W} + \frac{PrB_{II}^2}{2} \left[1 - \frac{I_O^2(K\bar{r})}{I_O^2(K)}\right] \right\} \tag{85}$$

Use of equation (64) then gives the temperature profile for fully developed flow, case II:

$$\bar{T}_\infty - \bar{T}_{\infty_W} = \frac{1}{2} Pr\ B_{II}^2 \left[1 - \frac{I_O^2(K\bar{r})}{I_O^2(K)}\right] \tag{86}$$

The distribution of $\bar{m}_\infty(\bar{r}) = N_O\bar{\rho}_\infty\bar{u}_\infty$ is

$$\bar{m}_\infty(\bar{r}) = \frac{\dfrac{\gamma}{\gamma-1} \bar{p}_\infty B_{II} \left[1 - \dfrac{I_O(K\bar{r})}{I_O(K)}\right]}{\bar{T}_{\infty_W} + \dfrac{1}{2} Pr\ B_{II}^2 \left[1 - \dfrac{I_O^2(K\bar{r})}{I_O^2(K)}\right]} \tag{87}$$

Case III ($\sigma = 0$)

It is of interest to investigate the limiting case where the electrical conductivity approaches zero, that is, the case of conventional gasdynamic pipe flow. If it is supposed that such a flow can become fully developed, the result from the momentum equations is

$$\bar{u}_\infty(\bar{r}) = \frac{1}{4} \left(-\frac{d\bar{p}_\infty}{d\bar{x}}\right) (1 - \bar{r}^2) \tag{88}$$

where $d\bar{p}_\infty/d\bar{x}$ is a constant. The energy equation and equation of state, (57) and (58), for this case (where $\bar{\Omega} = 0$) reduce to

$$\frac{1}{\gamma-1} \bar{u}_\infty \frac{d\bar{p}_\infty}{d\bar{x}} = \frac{\gamma}{\gamma-1} \frac{\bar{p}_\infty(\bar{x})}{Pr\ N_O} \left(\frac{1}{\bar{r}} v_\infty' + v_\infty''\right) + (\bar{u}_\infty')^2 \tag{89}$$

where $v_\infty = 1/\bar{\rho}_\infty$. Because $\bar{p}_\infty(\bar{x})$ is the only possible function of $\bar{x}$ in equation (89), it must be true that either $\bar{p}_\infty$ is a constant or $(1/Pr\ N_O)[(1/\bar{r})v_\infty' + v_\infty''] = 0$. Substitution of the latter consideration into equation (89) results in

$$(\bar{u}_\infty')^2 + \frac{1}{\gamma - 1}\left(-\frac{d\bar{p}_\infty}{d\bar{x}}\right) = 0$$

which is contradictory to the momentum equation, besides the fact that it implies that $\bar{u}_\infty'$ is imaginary if the necessary negative pressure gradient is assumed to exist. The only other possibility for fully developed flow, then, is $\bar{p}_\infty = $ constant. But then $d\bar{p}_\infty/d\bar{x} = 0$ and equation (88) then states that there is no flow. The conclusion is that it is not possible to have fully developed laminar flow in a pipe if the fluid is compressible unless the fluid particles are acted upon by body forces, that is, forces other than the surface forces due to pressure and friction. This is perhaps a surprising result because it is known that air flowing at low speed in a pipe does, at least very nearly, approach fully developed flow. But at low speeds viscous dissipation of energy is small and the flow is nearly incompressible. The momentum equations can then be satisfied without recourse to the energy equation; the pressure gradient is not required to be zero. (In the case where the fluid is not exactly incompressible, but small density changes with temperature, i.e., thermal expansion and contraction, are admitted, Maslen (ref. 12) has obtained solutions using an equation of state which is independent of pressure and using momentum and energy equations which involve a constant pressure gradient.) At high speeds, in addition to the fact that the density must be allowed to vary, there is greater viscous dissipation of energy, which fact lends to acceptance on physical grounds of the result found above, that a fully developed flow is not attained unless it is supported by a body force.

MASS-FLOW COMPARISON

In the section "Equations of Motion" physical arguments were given in support of the use of the hypothesis that $v_r \equiv 0$ and the consequent use of the function $\rho_O u_O(\partial u/\partial x)$ as an approximation for the term $\rho u(\partial u/\partial x)$ in the momentum equation. The approximation is, of course, exact at $x = 0$ because $(\rho u)_{x=0} = \rho_O u_O$. It is also true as x approaches infinity because $\partial u/\partial x$ approaches zero. Use of the approximation at values of x near zero is justified because, although u changes rapidly from u_O, the product ρu remains nearly at $\rho_O u_O$. At large values of x the approximation is good because $\partial u/\partial x$ becomes smaller and hence the term $\rho u(\partial u/\partial x)$ in the differential equation becomes less important. The approximation is least accurate at intermediate axial locations, that is, at values of x

where the center-line velocity is approximately intermediate between u_O and u_∞ and the product ρu is approximately intermediate between $\rho_O u_O$ and $\rho_\infty u_\infty$. One can obtain, therefore, an indication of the accuracy by comparing the mass flow at $x = \infty$ with the mass flow at $x = 0$, that is, by calculating the ratio $\overline{m}_\infty/\overline{m}_O$ versus $\overline{r}$. One can then consider the value of $\overline{m}/\overline{m}_O$ intermediate between $\overline{m}_\infty/\overline{m}_O$ and 1.0 to be a good indication of the accuracy of the approximation at the x location where it is least accurate. For this calculation equations (75) and (87) are used to find $\overline{m}_\infty$ for cases I and II, respectively, and $\overline{m}_O$ is equal to N_O.

First it must be required that over-all conservation of mass be satisfied. The respective expressions for $\overline{m}_\infty$ contain the parameters $\overline{p}_\infty$ and $\overline{T}_{\infty_W}$ which must have definite values depending upon the state of the flow at the pipe entry. Thus the various parameters must be related so that they satisfy the equation

$$\left. \begin{array}{c} \int_0^1 \overline{m}_O \overline{r} \, d\overline{r} = \int_0^1 \overline{m}_\infty \overline{r} \, d\overline{r} \\[2em] \frac{1}{2} N_O = \int_0^1 \overline{m}_\infty \overline{r} \, d\overline{r} \end{array} \right\} \qquad (90)$$

or

Case I (J_y = Constant)

For case I, the result of substituting equation (75) into (90) requires that the parameters be related by

$$\delta_1 = \ln \left\{ \frac{\delta_2}{\delta_2 + \delta_3 + \frac{1}{2}} \left[\frac{(1 + \delta_3 + \delta_4)(\delta_3 - \delta_4)}{(1 + \delta_3 - \delta_4)(\delta_3 + \delta_4)} \right]^{\frac{1+\delta_3}{\delta_4}} \right\} \qquad (91)$$

where

$$\delta_1 = \frac{N_O \left(\frac{\gamma - 1}{\gamma} \, \text{Pr} \right) (K^2 B_I)}{8 \overline{p}_\infty} \qquad (92)$$

$$\delta_2 = \frac{32 \overline{T}_{\infty_W}}{\text{Pr}(K^2 B_I)^2} = \frac{32}{\left(\frac{\gamma - 1}{\gamma} \, \text{Pr} \right) \gamma M_O^2} \frac{T_{\infty_W}/T_O}{(K^2 B_I)^2} \qquad (93)$$

$$\delta_3 = \frac{8}{K^2} \tag{94}$$

$$\delta_4 = \sqrt{\delta_3^2 + 2\delta_3 + 2\delta_2 + 1} \tag{95}$$

As will be discussed later, the results of calculations demonstrate the fact that

$$\overline{p}_0 - \overline{p}_\infty = \frac{N_0}{\gamma M_0^2} - \overline{p}_\infty = \frac{K^2 B_I}{3N_0} \tag{96}$$

Combination of equations (92) and (96) yields the relation

$$K^2 B_I = \frac{3N_0^2}{\gamma M_0^2} \frac{8\delta_1}{8\delta_1 + 3N_0^2 Pr(\gamma - 1)/\gamma} \tag{97}$$

From equations (91) and (97) a definite relationship between K^2 and $K^2 B_I$ can be seen for given values of N_0, $[(\gamma - 1)/\gamma]Pr$, γM_0^2, and T_{∞_W}/T_0. One may note that, for those cases where

$$K^2 B_I \ll 3N_0^2/\gamma M_0^2$$

equation (97) may be approximated by

$$K^2 B_I \approx \frac{8\delta_1}{\left(\frac{\gamma - 1}{\gamma} Pr\right)\left(\gamma M_0^2\right)}$$

and the relationship between $K^2 B_I$ and K^2 would then depend only on $[(\gamma - 1)/\gamma]Pr(\gamma M_0^2) \equiv (\mu/k)(u_0^2/T_0)$ and on T_{∞_W}/T_0. This is true, for example, if $N_0 > 100$, $K^2 B_I < 1000$ and γ and M_0 are of order unity.

The calculation can be made as follows: For various given values of K^2, N_0, $[(\gamma - 1)/\gamma]Pr$, and γM_0^2, a number of arbitrary values of δ_2 are specified. Corresponding to each of these values, then, δ_1 is known from equation (91). The values of $K^2 B_I$ are then found from equation (97), and the appropriate values of T_{∞_W}/T_0 are obtained from equation (93).

For chosen sets of the input parameters which satisfy equation (90), as calculated above, one may then calculate the quantity $\overline{m}_\infty/\overline{m}_0$ as a function of $\overline{r}$. Using equation (75), one obtains

$$\frac{\overline{m}_\infty}{\overline{m}_O} = \left(\frac{1}{\delta_1}\right) \left[\frac{1 - \overline{r}^2}{\delta_2 + \frac{1}{2}(1 - \overline{r}^4) + \delta_3(1 - \overline{r}^2)}\right] \tag{98}$$

Case II (E_y = Constant)

For case II, if equation (87) is substituted into equation (90), the required relationship among the parameters is found to be

$$\delta_5 = \int_O^1 \frac{(1 - \zeta)\overline{r}\,d\overline{r}}{\delta_6 + 1 - \zeta^2} \tag{99}$$

where

$$\zeta = \frac{I_O(K\overline{r})}{I_O(K)} \tag{100}$$

and where

$$\delta_5 = \frac{N_O\left(\frac{\gamma - 1}{\gamma}\right) Pr\, B_{II}}{4\overline{p}_\infty} \tag{101}$$

$$\delta_6 = \frac{2\,\overline{T}_{\infty W}}{Pr\, B_{II}^2} = \frac{2}{\left(\frac{\gamma - 1}{\gamma}Pr\right)\gamma M_O^2}\frac{T_{\infty W}/T_O}{B_{II}^2} \tag{102}$$

In this case the results of calculations, to be discussed later, reveal the fact that

$$\overline{p}_O - \overline{p}_\infty = \frac{N_O}{\gamma M_O^2} - \overline{p}_\infty = \frac{K^2(B_{II} - 1)}{3N_O} \tag{103}$$

Equations (101) and (103) may be combined to give an expression for B_{II}:

$$B_{II} = \frac{4\delta_5\left(\frac{3N_O^2}{\gamma M_O^2} + K^2\right)}{4\delta_5K^2 + 3N_O^2Pr\frac{\gamma - 1}{\gamma}} \tag{104}$$

For this case the calculation can be accomplished in a manner similar to that used in case I. For various given values of K^2, N_O, $[Pr(\gamma - 1)/\gamma]$, and γM_O^2, a number of arbitrary values of δ_6 are specified. Corresponding values of δ_5 are found from equation (99) (by numerical integration, for example), and then B_{II} is obtained from equation (104). The appropriate values of T_{∞_W}/T_O are obtained from equation (102).

Corresponding to the sets of input parameters which satisfy equation (90), as calculated above, $\overline{m}_\infty/\overline{m}_O$ may then be calculated. For this purpose equation (87) may be written:

$$\frac{\overline{m}_\infty}{\overline{m}_O} = \left(\frac{1}{2\delta_5}\right)\left(\frac{1 - \zeta}{\delta_6 + 1 - \zeta^2}\right) \tag{105}$$

where ζ is given by equation (100).

NUMERICAL EXAMPLES

The equations containing the infinite series solutions for the dimensionless velocity $\overline{u}$ and the dimensionless pressure $(\overline{p} - \overline{p}_\infty)$ at all $\overline{x}$ and $\overline{r}$ were programmed for evaluation on an IBM type 704 electronic data processing machine. Also calculated were the fully developed velocity and temperature profiles. The equations for both case I and case II were programmed.

A subroutine employing Newton's method as the iteration procedure was used to evaluate the eigenvalues, λ_n, as the successive roots of equation (33). An approximate value was found graphically for the first eigenvalue, λ_1. This approximate value was then used as a trial, or starting, value in the iteration procedure to solve for the actual value of λ_1. The trial value for the iteration in the vicinity of each succeeding eigenvalue, λ_n, was found by adding the number π to the preceding eigenvalue, λ_{n-1}.

The calculations were made for values of the Reynolds number N_O of 1000, 750, 500, and 250, values of K^2 of 1000, 500, 250, 100, 50, and 10, values of $B_I = (E_y/H_Ou_O) - (u/u_O) = J_yH_O/\sigma u_O H_O^2$ of 1.0 and 0.1 and values of $B_{II} = E_y/H_Ou_O$ of 100, 10, and 2. An appropriate range of $\overline{x}$ for each set of input parameters was used so that the asymptotic approach of the velocity distribution to the fully developed flow profile could be observed and so that the pressures near $\overline{x} = 0$ could be determined.

DISCUSSION OF RESULTS

Fully Developed Flow

The fully developed flow velocity, toward which the flow is assumed to accelerate starting from the inlet velocity, depends on K^2 and B_I for case I and on K^2 and B_{II} for case II. Plotted in figure 3 are the velocity profiles referenced to the value of the velocity on the pipe axis. As presented in this figure, the profile is independent of all parameters for case I. In this case the electromagnetic body force, which is balanced by the viscous forces in the fully developed flow, is constant over the cross section. The result, a parabolic profile, is the same as for the Hagen-Poiseuille incompressible pipe flow in which a constant pressure gradient maintains the flow. The velocity profiles depend on the Hartmann number K in case II. In this case the body force varies over the cross section. It is greater near the wall and thus tends to flatten the profile. As K approaches infinity, the body force approaches zero everywhere in the fully developed flow except in a boundary layer near the wall. Shown in figure 4 are curves of the fully developed flow center-line velocity versus K^2 for various values of the parameters B_I and B_{II}. In case I, where J_y is constant and the body force is constant and thus has a nonzero value in fully developed flow, the center-line velocity is directly proportional to K^2 as well as B_I. (The product $K^2 B_I$ is actually proportional to the ratio of the constant electric body force to the inlet viscous force on a fluid particle; that is, $K^2 B_I = F/(\mu u_0/a^2)$.) Thus, for this case, as the magnetic field is increased, the maximum velocity is also increased because the body force, which maintains a constant value throughout the entire flow, is increased. In case II the flow approaches the fully developed condition as the body force approaches a value proportional to $K^2 B_{II}/I_0(K)$ on the center line. Thus, for values of K near zero, the body force on the center line becomes proportional to $K^2 B_{II}$. But as K approaches infinity, the body force approaches zero. The fully developed flow center-line velocity is given by $u_\infty/u_0 = B_{II}[1 - 1/I_0(K)]$. Thus, as K nears zero, the fully developed flow velocity approaches zero. But as K approaches infinity, u_∞/u_0 approaches B_{II} (except very near the wall) and therefore becomes essentially independent of K.

The results for case II may be compared with those of Resler and Sears in their study of nonviscous one-dimensional magnetogasdynamic flow in a constant-area channel with no heat transfer (ref. 5). Resler and Sears distinguished essentially three basic types of flow (with respect to velocity): (1) choked flow, (2) smooth continuous acceleration (or deceleration), and (3) approach to an asymptotic state. When the viscosity is not zero, the flow properties (velocity, temperature, etc.) vary over the cross section, and the conditions which lead to choking as the velocity changes with x would therefore not be present over the entire cross section at any axial location. Hence the effects of choking are not evident in the present study and choked flow is not considered. Neither have the cases for which Resler and Sears found the flow to accelerate indefinitely with distance along the channel been investigated here.

Only those cases for which the flow velocity approaches the fully developed, or nonaccelerating unidirectional, flow state have been considered. The boundary condition was imposed that the flow asymptotically approach this state. For inviscid flow with no heat transfer, Resler and Sears found the asymptotic flow velocity to have the value E/H in some cases, while in others it was limited to $[(\gamma - 1)/\gamma]E/H$. If the effects of viscosity are small enough, the velocity and temperature profiles will be uniform, and hence one-dimensional, except in the boundary layer at the wall. All effects of viscosity and thermal conductivity will be confined to the boundary layer, and the flow outside the boundary layer will be governed by the inviscid flow equations of Resler and Sears. Thus, if $u_0 < [(\gamma - 1)/\gamma]E/H < E/H$, as the velocity outside the boundary layer approaches the value $[(\gamma - 1)/\gamma]E/H$, the flow will indeed cease to accelerate and hence the velocity will become asymptotic to $[(\gamma - 1)/\gamma]E/H$. In the present analysis (case II), if the viscosity is assumed to approach zero, then the Hartmann number becomes infinite and the flow does become essentially one-dimensional, except for the boundary layer near the wall (see fig. 4), and both of the asymptotic flow cases indicated by Resler and Sears ($u \to E/H$ and $u \to [(\gamma - 1)/\gamma]E/H$) are shown to be possible solutions of the fully developed flow equations, under the proper respective conditions, in the limit as K approaches infinity (see eqs. (80) and (83)). However, if K is small enough that the velocity profile is not extremely flat, then the first-order differential equations of Resler and Sears do not apply, and the only possible asymptotic flow velocity is that given by equation (83). The effects of heat conduction will not permit the flow to become fully developed as the velocity approaches $[(\gamma - 1)/\gamma]E_y/H_0$, and hence the flow will continue to accelerate until the center-line velocity approaches asymptotically the value, $(E_y/H_0)[1 - 1/I_0(K)]$ (provided the proper constant wall temperature is supplied). As noted, however, the limiting results for inviscid flow agree completely with the asymptotic flow cases discussed by Resler and Sears.

The temperature distributions in fully developed flow are shown plotted in figure 5. The results, as presented here in dimensionless form and in terms of the various parameters as indicated, depend only on Hartmann number, K. The temperatures are referenced to the constant wall temperature. It is seen that the temperature profiles are governed to a great extent by the nature of the distribution of Joule heating. The effects of the various parameters on the temperature profiles are very similar to their effects on the velocity profiles. In case I the Joule heating is everywhere constant. As K approaches zero, the temperature profiles approach parabolic shape. As K goes to infinity, the shape becomes proportional to $[1 - (r/a)^4]$. Because the Joule heating is nowhere zero in the fully developed flow for this case, the temperature continues to increase as K increases. The Joule heating in case II varies over the cross section, being greater near the wall. As K approaches zero, the temperature difference $(T - T_w)$ approaches zero. As K approaches infinity, the Joule heating approaches zero everywhere except in the boundary layer, and thus the temperature profiles approach a uniform profile.

Velocity in the Accelerating Portion of the Flow

The development of the velocity profile from the uniform profile at the pipe inlet is illustrated by several examples in figures 6 and 7. Figure 6 gives examples corresponding to case I. For all cases here, the flow develops, starting with a thin boundary layer near the inlet, to the parabolic profile of fully developed flow (although the parabolic shape is not evident from the semilog plots of fig. 6). The effects of the various parameters will best be observed by studying the center-line velocities, as the radial development is very similar for all cases. It will be noted, however, that figures 6(b) and 6(c) are identical because these results depend only on N_O and on the product of K^2 and B_I in case I. Figure 7 illustrates case II. For high values of K, the boundary layer remains thin, but as K decreases, the boundary layer develops into a profile approaching a parabolic shape.

The center-line velocity distribution along the axial coordinate in the accelerating portion of the flow is a function of the inlet Reynolds number N_O and the product $K^2 B_I$ for case I; in case II it depends on the values of N_O, K^2, and B_{II}. Figure 8 shows the center-line velocity relative to the inlet velocity. It is noted here that for small values of $K^2 B_I$ in case I, the velocity overshoots the fully developed flow velocity before approaching it asymptotically. In the accelerating flow, as in the fully developed flow, the body force in case I is constant; whereas in case II, it varies with axial distance as well as over the cross section. Thus the body force in case II is greater near the inlet than near the fully developed flow, where it approaches zero as K approaches infinity. Nevertheless, the center-line velocity change in the accelerating portion seems to behave nearly the same in case I as in case II; that is, the shapes of the curves are nearly the same. It is noted, however, that increasing K in case II causes faster acceleration toward fully developed flow, an effect which is not seen in case I because increasing K in case I also increases the fully developed flow velocity. In figure 9 the center-line velocity distributions are shown relative to the fully developed flow velocity. Figure 9(a) shows the effect of varying K^2 and B_I for case I with N_O having the value 1000. As $K^2 B_I$ approaches infinity the axial velocity distribution, in the form presented in figure 9(a), approaches a single curve. One will note that the curve for $K^2 B_I = 1000$ cannot be distinguished from that for $K^2 B_I = 500$. In figure 9(b) can be seen the effect of varying N_O in case I. Higher values of N_O cause the velocity to approach the asymptotic profile more slowly, that is, the fluid proceeds further along the pipe before the flow becomes fully developed. The effect of varying K^2 and B_{II} for case II is given in part (c). Increasing K^2 causes the flow to approach the fully developed condition more rapidly. Higher values of B_{II} cause the flow to reach the fully developed state more slowly because the fluid must accelerate to higher velocity. Part (d) shows that the effect of varying N_O in case II is essentially the same as for case I.

From an expanded plot similar to those used in figure 9 can be read the values of x^*/a; that is, the values of x/a where the center-line flow velocity has reached a value within 1 percent of the fully developed flow velocity. It was found that the best type of plot for this purpose was one of $\log |1 - (u/u_\infty)_{r=0}|$ versus $(1/N_0)(x/a)$ for case I and $\log [1 - (u/u_\infty)_{r=0}]$ versus $(K^2/N_0)(x/a)$ for case II. On these plots the results were very nearly straight lines, except for portions of the curves for the "overshoot" cases of case I. When the results for x^* in case I are plotted as indicated in part (a) of figure 10, they fall on a single curve for all values of N_0 in the range 250 to 1000. It is seen then that x^*/a is directly proportional to N_0 and, at high values of the product K^2B_I, it becomes nearly independent of K^2B_I. As K^2B_I decreases to low values, near 4.0, x^*/a also decreases. The reason for this is that the fully developed flow velocity is also directly proportional to K^2B_I, and is equal to $(1/4)K^2B_I$ on the pipe axis. Thus, as K^2B_I decreases, the pipe length required to achieve the fully developed flow velocity on the axis decreases because the velocity change is decreased. In fact, when K^2B_I is very small, the fluid decelerates to fully developed flow, and, as K^2B_I approaches zero, the value of x^*/a rises again and approaches infinity, because the flow must approach zero velocity because of the requirement of zero pressure gradient in the fully developed flow. For case II, plotting the results in the manner shown in figure 10(b) brings them to the same order of magnitude for the values of the input parameters used. It is seen that, for high N_0, x^*/a is nearly directly proportional to N_0. It decreases with increase in K^2 because the body force is then higher near the inlet, but lower near the fully developed flow. In fact, for this case, x^*/a is nearly inversely proportional to K^2 for fairly high values of K^2. It increases with increase in B_{II} (for B_{II} greater than unity) because the final velocity approached is higher. As B_{II} decreases from unity to zero, the value of x^*/a must approach infinity because the fully developed flow velocity approaches zero and the fluid must then decelerate from the inlet velocity to zero. These results for both cases I and II support the conclusions reached in the study of the energy equation in a previous section; that is, compressible viscous flow cannot become fully developed unless it is supported by a body force. Thus as K^2, B_I, and B_{II}, the significant parameters involved in the strength of the body force, approach zero, the pipe length required to achieve fully developed flow goes to infinity.

Values of x^*/a in case I are, in general, higher than those in case II. In case I the flow takes longer to become fully developed because the body force is applied at a constant rate along the tube, and energy is being added to the flow through Joule heating at a constant rate. In case II the flow becomes fully developed more rapidly because both the body force and the energy added by Joule heating decrease as the velocity increases toward the fully developed flow value.

Pressure in the Accelerating Portion of the Flow

The center-line pressure distribution over the axial distance is shown in figure 11. The results are calculated from equation (44) using $\overline{r} = 0$ and the fact that

$$\overline{p} - \overline{p}_\infty = N_O \left(\frac{p - p_\infty}{\rho_O u_O{}^2} \right)$$

When the results for case I are plotted in the manner illustrated in figure 11(a), they are found to be nearly independent of N_O for values of N_O in the range 250 to 1000. Results are shown for various values of the product $K^2 B_I$. It is seen that as $K^2 B_I$ increases, the results as plotted here approach a single curve, and thus that the pressure distribution becomes proportional to $K^2 B_I$, or to the body force. For case II (fig. 11(b)) the results for N_O in the range 250 to 1000, K^2 in the range 50 to 1000, and B_{II} in the range 2 to 100 fall on a single curve.

The pressure difference between the value at the pipe inlet and the fully developed flow value can be found by observing the value approached as x approaches zero in figure 11. It is noted that on both parts of figure 11, all curves approach the value 1/3 on the ordinate and therefore that the value of $(p_0-p_\infty)/\rho_O u_O{}^2$ is $(1/3)K^2 B_I/N_O{}^2$ for case I and is equal to $(1/3)K^2(B_{II} - 1)/N_O{}^2$ in case II. Thus the difference between the pressure at the inlet and that in the fully developed flow can be calculated directly. Although the relationships among the various parameters are obvious from these formulas, numerical results are presented in figure 12 to show the order of magnitude of the pressure difference for various values of the parameters. It is seen that the pressure differences required are in most cases very small compared to the inlet dynamic pressure. It must be noted that for a given set of input parameters, N_O, K, and B_I or B_{II}, there is a definite pressure difference. Thus, if this pressure difference does not exist in the actual flow situation, then the indication is that the fully developed flow condition will not be attained.

Results of the Mass-Flow Comparison

For the purpose of obtaining an indication of the accuracy of using $\rho_O u_O(\partial u/\partial x)$ as an approximation for the term $\rho u(\partial u/\partial x)$ in the momentum equation, the dimensionless mass-flow profile in fully developed flow, $\overline{m}_\infty$, may be compared with the dimensionless inlet mass flow, $\overline{m}_O$, as discussed in a previous section, "Mass-Flow Comparison." Shown in figures 13(a) and 13(b), respectively, are examples of the required relationships among the parameters for case I and case II, which must

first be calculated (in order that over-all conservation of mass be satisfied). Note that although the examples plotted in figure 13(a) were calculated for $N_O = 1000$, the results are essentially independent of N_O for the ranges of parameters used if N_O is greater than a number substantially less than 100. The results shown therefore also correspond to any combination of values for γM_O^2 and $[Pr(\gamma - 1)/\gamma]$ which have the same product as those listed. (See earlier text under "Mass-Flow Comparison.")

Figures 14(a) and 14(b) show examples of $\bar{m}_\infty/\bar{m}_O$ versus $\bar{r}$ corresponding to several of the relationships given in figure 13. Some specific examples to which the cases plotted in figure 14 correspond are listed in tables I and II. For these typical example cases and from the considerations outlined under the section "Mass-Flow Comparison," one can determine for which sets of conditions the approximation under consideration is most valid. (Recall that the approximation is most correct for those cases where m/m_O is near unity.) Evidently the validity increases as one progresses through cases I through 4 for case I (see table I) and through cases 5 through 7 for case II (see table II).

CONCLUDING REMARKS

It has been found that for the occurrence of fully developed laminar flow of a compressible viscous fluid in a pipe, an axial body force must be applied. That is, the viscous forces must be balanced by fluid body forces rather than simply by forces due to a thermodynamic pressure difference. It is thus found that, as the effects producing the body forces are decreased to zero, the pipe length required for fully developed flow becomes infinite.

It is also shown that, for the flow of a compressible viscous fluid to become fully developed, the wall temperature must approach a constant value, and it is seen that definite values of the pressure difference between the value at the inlet and the constant value in fully developed flow are required in order that the fully developed flow be smoothly obtained. The radial temperature distribution is also seen to approach an asymptotic profile.

In the application of the solutions to the magnetogasdynamic pipe flow problem, in which the axial body force is the "electric body force," the flow results depend on the nature of the electric field and current density. Two special cases have been studied in this report: In case I the component of current density perpendicular to the velocity and the magnetic field is assumed constant. For this case the velocity profiles approach parabolic shape as the flow approaches the fully developed condition. The temperature in the fully developed flow is found to depend on the Hartmann number. As Hartmann number, K, approaches infinity, the temperatures become proportional to the fourth power of K, and as K

approaches zero, the radial temperature profile becomes parabolic and proportional to the square of K. The pipe length required to achieve a velocity within 1 percent of fully developed flow velocity is found to approach a value proportional to the inlet Reynolds number for high values of the Hartmann number. The pipe lengths are in the order of hundreds of radii for a Reynolds number of 1000. The difference between the pressure at the inlet and that in the fully developed flow is found to be very small in comparison to the inlet dynamic pressure, the ratio being proportional to the ratio of the constant electromagnetic body force to the inlet viscous force on a fluid particle and inversely proportional to the square of the inlet Reynolds number. In case II the component of the electric field perpendicular to the velocity and the magnetic field is considered constant throughout the flow field. The velocity profiles for this case approach fully developed flow profiles which become flatter with increase in Hartmann number. As the viscosity approaches zero (Hartmann number approaches infinity), the results approach those of the inviscid constant-area channel flow studied by Resler and Sears. In contrast to the two different values of the asymptotic velocity indicated by Resler and Sears for inviscid flow, it is shown that only one asymptotic flow velocity profile is possible for a given set of conditions when the effects of viscosity are significant, which profile corresponds to the upper limit indicated by Resler and Sears, modified by the Hartmann number. The fully developed flow temperature profiles for case II behave much like the velocity profiles. For high values of the Hartmann number, the entry pipe length is nearly proportional to the ratio of inlet Reynolds number to the square of the Hartmann number. It also increases as the ratio of the electric field to the product of the magnetic field and inlet velocity increases. The pipe lengths are in the order of 5 radii for Reynolds number of 1000 and Hartmann number equal to $\sqrt{1000}$. In case II the difference between the pressure at the inlet and that in the fully developed flow is also found to be small, in general, compared to the inlet dynamic pressure. The ratio of the pressure difference to the inlet dynamic pressure is proportional to the ratio of electromagnetic body force at the pipe inlet to the inlet viscous force on a fluid particle and inversely proportional to the square of the inlet Reynolds number.

Ames Research Center
    National Aeronautics and Space Administration
        Moffett Field, Calif., Feb. 13, 1961

APPENDIX A

EVALUATION OF THE CONSTANT α FOR THE FLOW

DEVELOPMENT FROM A UNIFORM PROFILE

The solutions to the equations of motion corresponding to the constant of integration, α, in equation (29) having the value zero have been given in the text of this report. The possibility of solutions for α having a value other than zero will be investigated in this appendix.

If α is assumed to have a nonzero value, application of conditions (30a) and (30b) to equation (31) gives the result

$$R_n = \frac{-\alpha}{\lambda_n^2} \left[\frac{J_0(\lambda_n \overline{r})}{J_0(\lambda_n)} - 1 \right] \tag{A1}$$

where the values of α and the eigenvalues λ_n are, as yet, undetermined. It will be seen that α need not be determined directly, since it automatically falls out of the equations. Equation (A1) may be substituted into equation (26) to give

$$U(\overline{x}, \overline{r}) = \sum_{n=1}^{\infty} B_n e^{\epsilon_n \overline{x}} \left[\frac{J_0(\lambda_n \overline{r})}{J_0(\lambda_n)} - 1 \right] \tag{A2}$$

where

$$B_n = \left(\frac{-\alpha}{\lambda_n^2} \right) A_n \tag{A3}$$

Application of boundary condition (25a) to equation (A2) then leads to the result

$$\overline{\xi}(\overline{r}) = \sum_{n=1}^{\infty} D_n J_0(\lambda_n \overline{r}) \tag{A4}$$

where

$$\overline{\xi}(\overline{r}) = \overline{u}_\infty(\overline{r}) - 1 + \sum_{n=1}^{\infty} B_n , \qquad (0 \leq \overline{r} < 1) \tag{A5}$$

and where

$$D_n = \frac{B_n}{J_0(\lambda_n)} \tag{A6}$$

If the functions $J_0(\lambda_n \bar{r})$ are orthogonal, then equation (A4) represents the expansion of the function $\bar{\xi}(\bar{r})$ in a series of orthogonal eigenfunctions. In order for $J_0(\lambda_n \bar{r})$ to be orthogonal, one of the three possible orthogonality conditions must be satisfied (see ref. 15). The most general of the three is

$$\beta J_0(\lambda_n) + \lambda_n J_1(\lambda_n) = 0 \tag{A7}$$

where β is a negative constant. It will be noted that the other two possible conditions, $J_0(\lambda_n) = 0$ and $J_1(\lambda_n) = 0$, are merely special cases of equation (A7), that is, the respective cases where $\beta = -\infty$ and $\beta = 0$. The case where $\beta = 0$ must be ruled out because this would impose the condition, through equation (A2), that $\partial U(\bar{x},1)/\partial \bar{r} = 0$. This requires the restriction that at the wall $\partial \bar{u}/\partial \bar{r} = \bar{u}_\infty{}'(1)$ at all $\bar{x}$, which is unreasonable for the case of a uniform velocity profile at the inlet. The case $\beta = -\infty$ corresponds to $\alpha = 0$, which case has been discussed in the text.

The choice of various finite negative values of β in equation (A7) would supposedly result in different physical conditions of the problem. For example the difference in pressure at two points in the flow would be a function of the choice of β. Thus a complete set of eigenvalues are prescribed as the roots of equation (A7) with a given choice of β, and the appropriate pressure distribution would result.

The coefficients D_n may then be determined by the conventional method:

$$D_n = \frac{\int_0^1 \bar{\xi}(\bar{r}) J_0(\lambda_n \bar{r}) \bar{r} \, d\bar{r}}{\int_0^1 [J_0(\lambda_n \bar{r})]^2 \bar{r} \, d\bar{r}} \tag{A8}$$

Case I $(\bar{F} = K^2 B_I)$

For case I, using equations (19), (A5), (A6), and (A8) gives the result

$$D_n = \left(\sum_{n=1}^\infty B_n - 1 \right) f + A \left(\frac{4f}{\lambda_n{}^2} - fg \right) \tag{A9}$$

where

$$f = f(\lambda_n) = \frac{2J_1(\lambda_n)}{\lambda_n [J_0(\lambda_n)]^2 + \lambda_n [J_1(\lambda_n)]^2} \tag{A10}$$

and

$$g = g(\lambda_n) = \frac{2 J_0(\lambda_n)}{\lambda_n J_1(\lambda_n)} \tag{A11}$$

If the sum over values of n from one to infinity is taken of equation (A9), there results

$$\sum_{n=1}^{\infty} D_n = \left(\sum_{n=1}^{\infty} f \right) \left(\sum_{n=1}^{\infty} B_n - 1 \right) + A \sum_{n=1}^{\infty} \left(\frac{4f}{\lambda_n^2} - fg \right)$$

If $\bar{r} = 0$ is substituted into equations (A4) and (A5), using equation (19), the following relation is found:

$$\sum_{n=1}^{\infty} D_n = A + \left(\sum_{n=1}^{\infty} B_n - 1 \right)$$

If the above two relations for $\sum_{n=1}^{\infty} D_n$ are equated, the following expression results:

$$\sum_{n=1}^{\infty} B_n - 1 = A \left[\frac{\sum_{n=1}^{\infty} \left(\frac{4f}{\lambda_n^2} - fg \right) - 1}{1 - \sum_{n=1}^{\infty} f} \right] \tag{A12}$$

Substitution of equation (A12) into equation (A9), making use of equations (A7), (A10), and (A11), gives the result

$$B_n = \frac{2A}{\lambda_n^2 + \beta^2} \left(\frac{\beta - 2 + 8\beta^2 S_2}{1 + 2\beta S_1} - \frac{4\beta}{\lambda_n^2} \right) \tag{A13}$$

where

$$S_1 = \sum_{n=1}^{\infty} \left[\frac{1/J_0(\lambda_n)}{\lambda_n^2 + \beta^2} \right] \tag{A14}$$

and

$$S_2 = \sum_{n=1}^{\infty} \left[\frac{1/J_0(\lambda_n)}{\lambda_n^2(\lambda_n^2 + \beta^2)} \right] \tag{A15}$$

There are two indications that this solution which has been found for $\alpha \neq 0$ is not possible. First, it is found by computing S_1 and S_2 that $S_1 = -1/2\beta$ and that $S_2 = (2 - \beta)/8\beta^2$. Therefore the first term inside the bracket in equation (A13) is indeterminate, that is, both the numerator and denominator of that term are identically zero for all β. The second indication is seen by comparing equation (A9) with equation (A13), using also equation (A6). The entire right side of equation (A13) has the independent parameter A as a factor. Therefore, in order that equation (A13) be compatible with equation (A9), it must be true that either (1) $\sum\limits_{n=1}^{\infty} B_n = 1$, or (2) $\left[\sum\limits_{n=1}^{\infty} B_n - 1\right]$ must have a factor A. The first consideration cannot be true because, from equation (A13), B_n has a factor A. Therefore, $\sum\limits_{n=1}^{\infty} B_n$ would also necessarily have a factor A.

This same point rules out the second consideration because if $\sum\limits_{n=1}^{\infty} B_n$ has a factor A, then $\left[\sum\limits_{n=1}^{\infty} B_n - 1\right]$ cannot have a factor A. It is therefore shown for case I that the solutions corresponding to values of α unequal to zero are not possible.

<center>Case II $[\overline{F} = K^2(B_{II} - \overline{u})]$</center>

For case II, equations (48), (A5), (A6), and (A8) lead to

$$D_n = \left(\sum_{n=1}^{\infty} B_n - 1\right) f + Cfh \tag{A16}$$

where $f = f(\lambda_n)$ is given by equation (A10) and

$$h = h(\lambda_n) = 1 - \left(\frac{\lambda_n^2}{\lambda_n^2 + K^2}\right)\left[K \frac{I_1(K)}{I_0(K)} \frac{J_0(\lambda_n)}{\lambda_n J_1(\lambda_n)} + 1\right] \tag{A17}$$

If the sum over values of n from one to infinity is taken of equation (A16), a relation for $\sum\limits_{n=1}^{\infty} D_n$ results which may be equated to another

relation for $\displaystyle\sum_{n=1}^{\infty} D_n$ found by substituting $\bar{r} = 0$ into equations (A4) and (A5). A resulting expression is

$$\sum_{n=1}^{\infty} B_n - 1 = \frac{C\left[\displaystyle\sum_{n=1}^{\infty} fh - 1 + 1/I_0(K)\right]}{1 - \displaystyle\sum_{n=1}^{\infty} f} \tag{A18}$$

Substitution of equation (A18) into (A16), using (A7), (A10), and (A17), results in

$$B_n = C\left(\frac{2\beta}{\lambda_n^2 + \beta^2}\right)\left[\frac{1 + 2\beta S_3 - 1/I_0(K)}{1 + 2\beta S_1} - \frac{K^2 + (1/\beta)\lambda_n^2 K I_1(K)/I_0(K)}{K^2 + \lambda_n^2}\right] \tag{A19}$$

where S_1 is given by equation (A14) and where

$$S_3 = \sum_{n=1}^{\infty} \frac{\dfrac{K^2 + (1/\beta)\lambda_n^2 K I_1(K)/I_0(K)}{K^2 + \lambda_n^2}}{J_0(\lambda_n)(\lambda_n^2 + \beta^2)} \tag{A20}$$

Equations (A16) and (A19) may be compared, with the same object in mind as was considered in case I, to show that they are not compatible, and therefore that solutions corresponding to values of α unequal to zero are not possible for case II.

REFERENCES

1. von Kármán, T.: Applications of Magnetofluidmechanics. Astronautics, vol. 4, no. 10, Oct. 1959, p. 30.

2. Patrick, R. M.: A Description of a Propulsive Device Which Employs a Magnetic Field as the Driving Force. Avco Res. Lab., Res. Rep. 28, May 1958.

3. Ghai, M. L.: Plasma Propulsion for Space Applications. General Electric Company, Flight Propulsion Lab. Dept. Paper Presented to ARDC-OSR Contractors Conference on Ion and Plasma Research, Oct. 1, 1958.

4. Resler, E. L., and Sears, W. R.: The Prospects for Magneto-Aerodynamics. Jour. Aero. Sci., vol. 25, no. 4, April 1958, pp. 235-245.

5. Resler, E. L., and Sears, W. R.: Magneto-Gasdynamic Channel Flow. Zeitschrift für Angewandte Mathematik und Physik, vol. IXb, 1958, pp. 509-518.

6. Shercliff, J. A.: Entry of Conducting and Non-conducting Fluids in Pipes. Proc. Cambridge Philos. Soc., vol. 52, pt. 3 July 1956, pp. 573-583.

7. Shercliff, J. A.: Some Engineering Applications of Magnetohydrodynamics. Proc. Royal Soc. of London, vol. 233, no. 1194, 29 Dec. 1955, pp. 396-401.

8. Shercliff, J. A.: The Flow of Conducting Fluids in Circular Pipes Under Transverse Magnetic Fields. Jour. Fluid Mech., vol. 1, pt. 6, Dec. 1956, pp. 644-666.

9. Sears, W. R.: Magnetchydrodynamic Effects in Aerodynamic Flows. ARS Jour., vol. 29, no. 6, June 1959, pp. 397-406.

10. Rossow, Vernon J.: On Series Expansions in Magnetic Reynolds Number. NASA TN D-10, 1959.

11. Schlichting, H.: Boundary Layer Theory. McGraw-Hill Book Co., New York, 1955, pp. 10-12, 62-64.

12. Maslen, Stephen H.: On Fully Developed Channel Flows: Some Solutions and Limitations, and Effects of Compressibility, Variable Properties, and Body Forces. NASA TR R-34, 1959.

44

13. Hains, F. D., and Yoler, Y. A.: Axi-Symmetric Magneto-Gas Dynamic
       Channel Flow. Rep. 12, Flight Sciences Lab., Boeing Airplane Co.,
       Aug. 1959.

14. Cowling, T. G.: Magnetohydrodynamics. New York, Interscience Pub.,
       Inc., 1957, p. 10.

15. Hildebrand, F. B.: Advanced Calculus for Engineers. Prentice-Hall,
       Inc., New York, 1949, pp. 224-232, 248-254.

16. McLachlan, N. W.: Bessel Functions for Engineers. Oxford Univ. Press,
       London, 1941, pp. 94-95.

17. Wu, Ching-Sheng: On the Energy Equation in Magnetogasdynamics. Tech.
       Rep. No. 32-2, Jet Propulsion Laboratory, Calif. Inst. of Technology,
       Pasadena, Calif., Jan. 7, 1960.

A
3
9
6

A
3
9
6

TABLE I.- EXAMPLES OF CASES PLOTTED IN FIGURE 14(a) FOR CASE I
$(J_y = \text{CONSTANT})$, $(N_O = 1000)$

Case	δ_2	K^2	γM_O^2	$\dfrac{\gamma-1}{\gamma}\,Pr$	$K^2 B_I$	$\dfrac{T_W}{T_O}$
1	10^2	10^3	1	0.10	0.39832	0.49580×10^{-1}
			1	.25	.15933	$.19832\times10^{-1}$
			5	.10	.079664	$.99162\times10^{-2}$
			5	.25	.031865	$.39664\times10^{-2}$
2	10^2	10	1	.10	.39624	$.49064\times10^{-1}$
			1	.25	.15850	$.19626\times10^{-1}$
			5	.10	.079248	$.98129\times10^{-2}$
			5	.25	.031699	$.39251\times10^{-2}$
3	1.0	10^3	1	.10	28.288	2.5007
			1	.25	11.315	1.0003
			5	.10	5.6577	.50014
			5	.25	2.2631	.20006
4	1.0	10	1	.10	21.046	1.3842
			1	.25	8.4186	.55369
			5	.10	4.2093	.27684
			5	.25	1.6837	.11074

TABLE II.- EXAMPLES OF CASES PLOTTED IN FIGURE 14(b) FOR CASE II
$(E_y = \text{CONSTANT})$

Case	δ_6	K^2	N_O	γM_O^2	$\dfrac{\gamma-1}{\gamma}\,Pr$	B_{II}	$\dfrac{T_W}{T_O}$
5	1.0	10	1000	1.0	.10	5.3889	1.4520
				1.0	.25	2.1556	.58082
			100	1.0	.10	5.3811	1.4478
				1.0	.25	2.1548	.58038
6	1.0	100	1000	1.0	.10	8.2955	3.4408
				1.0	.25	3.3188	1.3768
			100	1.0	.10	8.1011	3.2814
				1.0	.25	3.2936	1.3560
7	1.0	1000	1000	1.0	.10	9.4137	4.4309
				1.0	.25	3.7726	1.7791
			100	1.0	.10	7.4200	2.7528
				1.0	.25	3.4657	1.5014
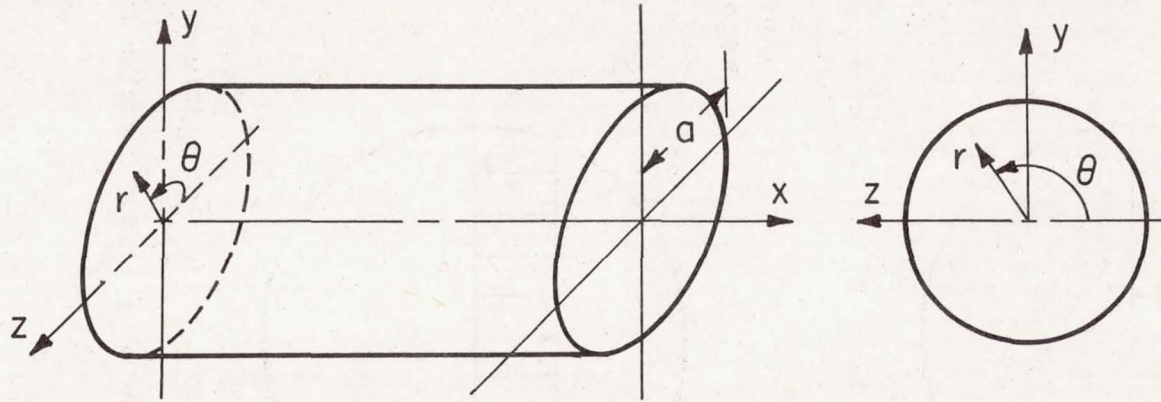
Figure 1.- Coordinate system.

Component of
current density, J_y

Uniform applied
magnetic field, H_0
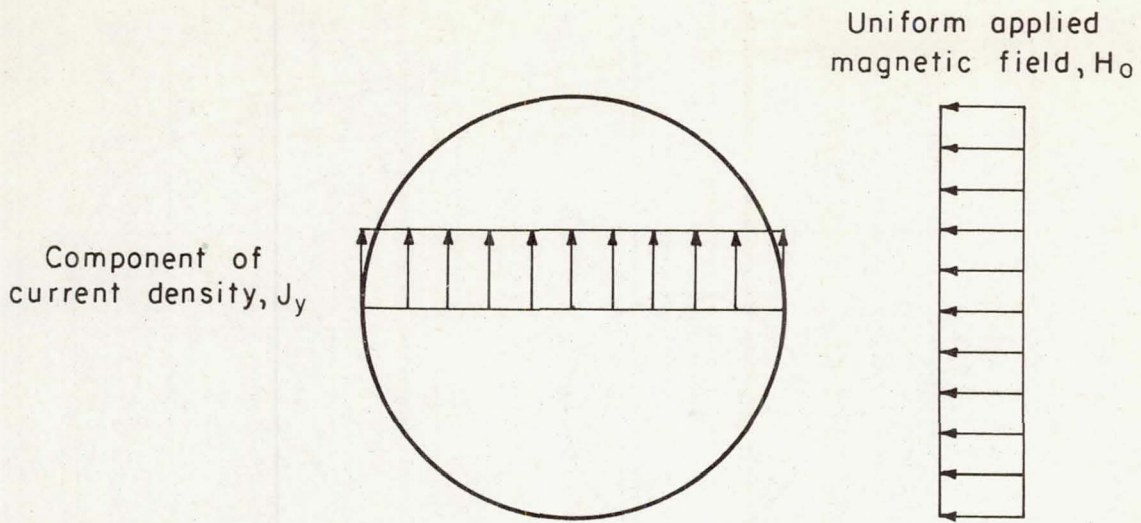
(a) Case I (J_y = constant; E_y to be determined).

Component of
electric field, E_y

Uniform applied
magnetic field, H_0
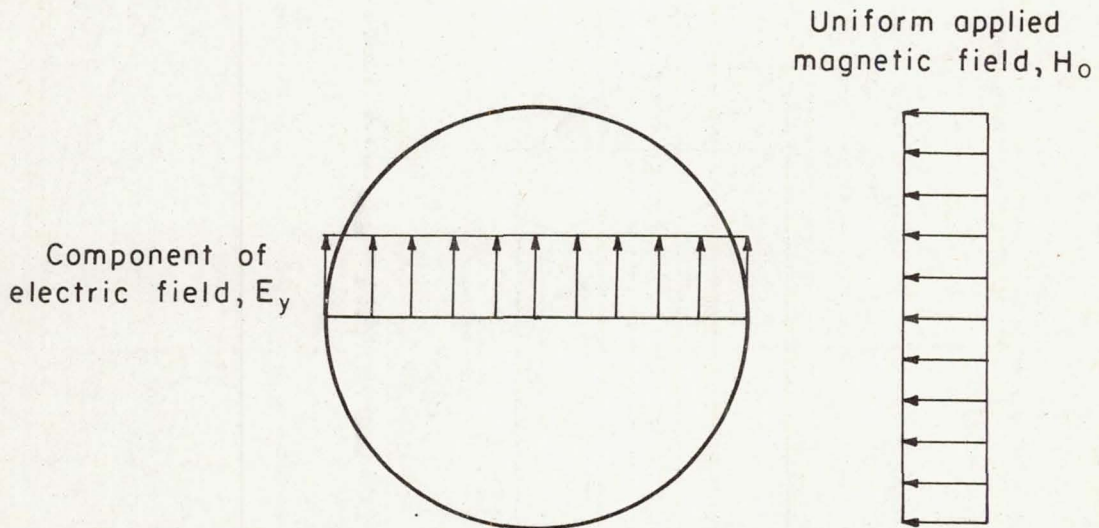
(b) Case II (E_y = constant; J_y to be determined).

Figure 2.- Configuration of electromagnetic fields.
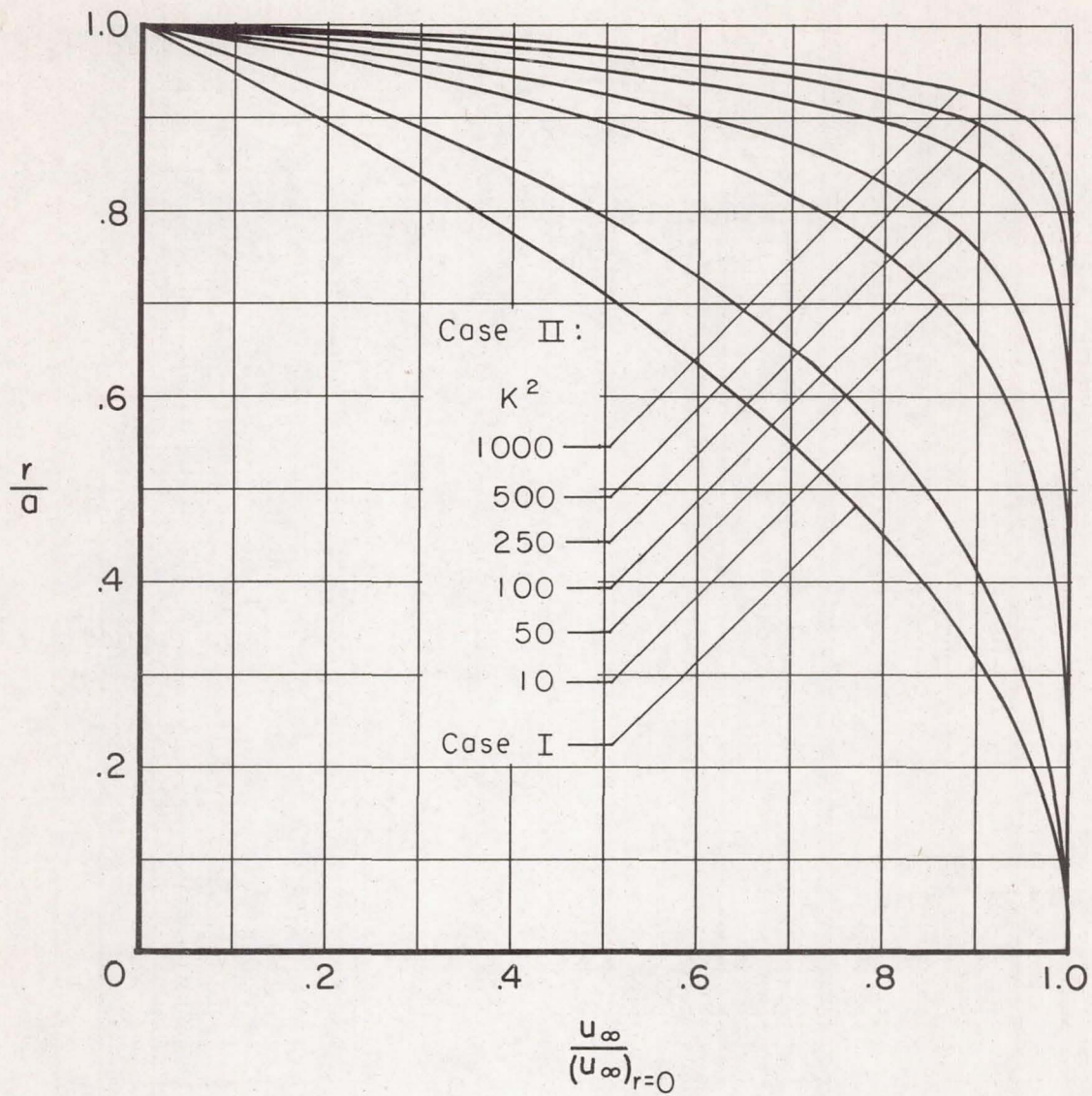
Figure 3.- Fully developed flow velocity profiles.

50
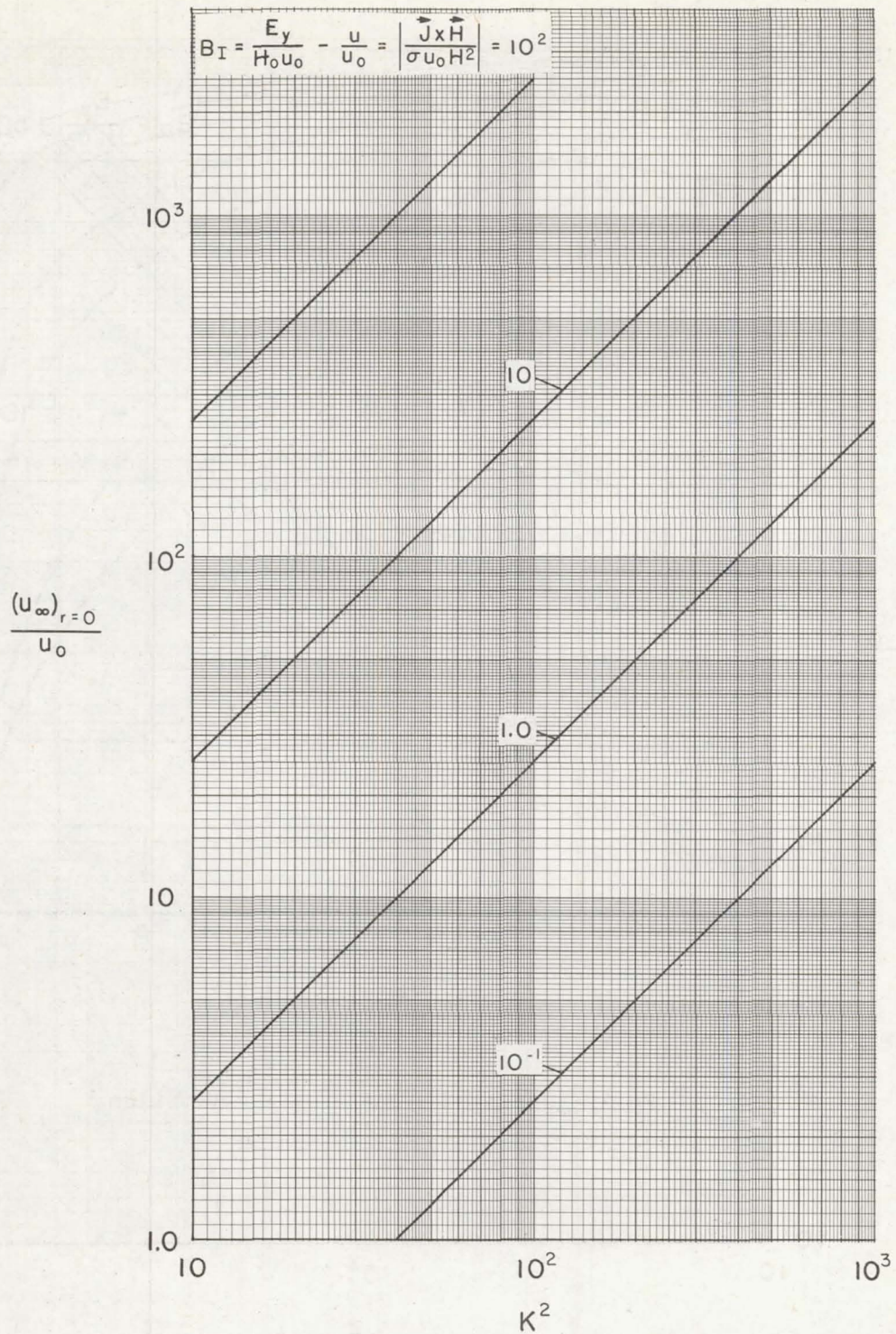
(a) Case I.

Figure 4.- Fully developed flow center-line velocity.

$$B_{II} = \frac{E_y}{H_0 u_0} = 500$$
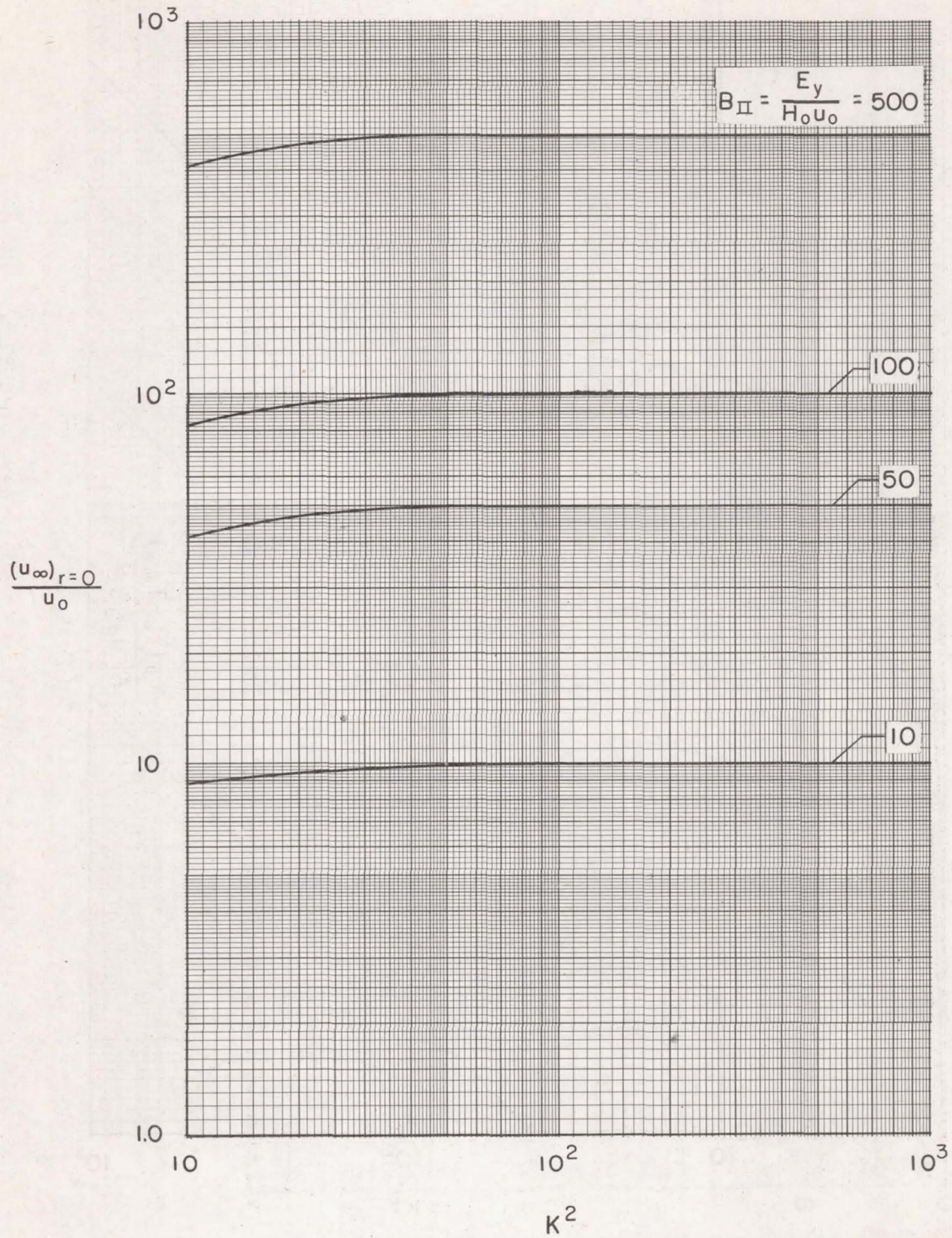
(b) Case II.

Figure 4.- Concluded.
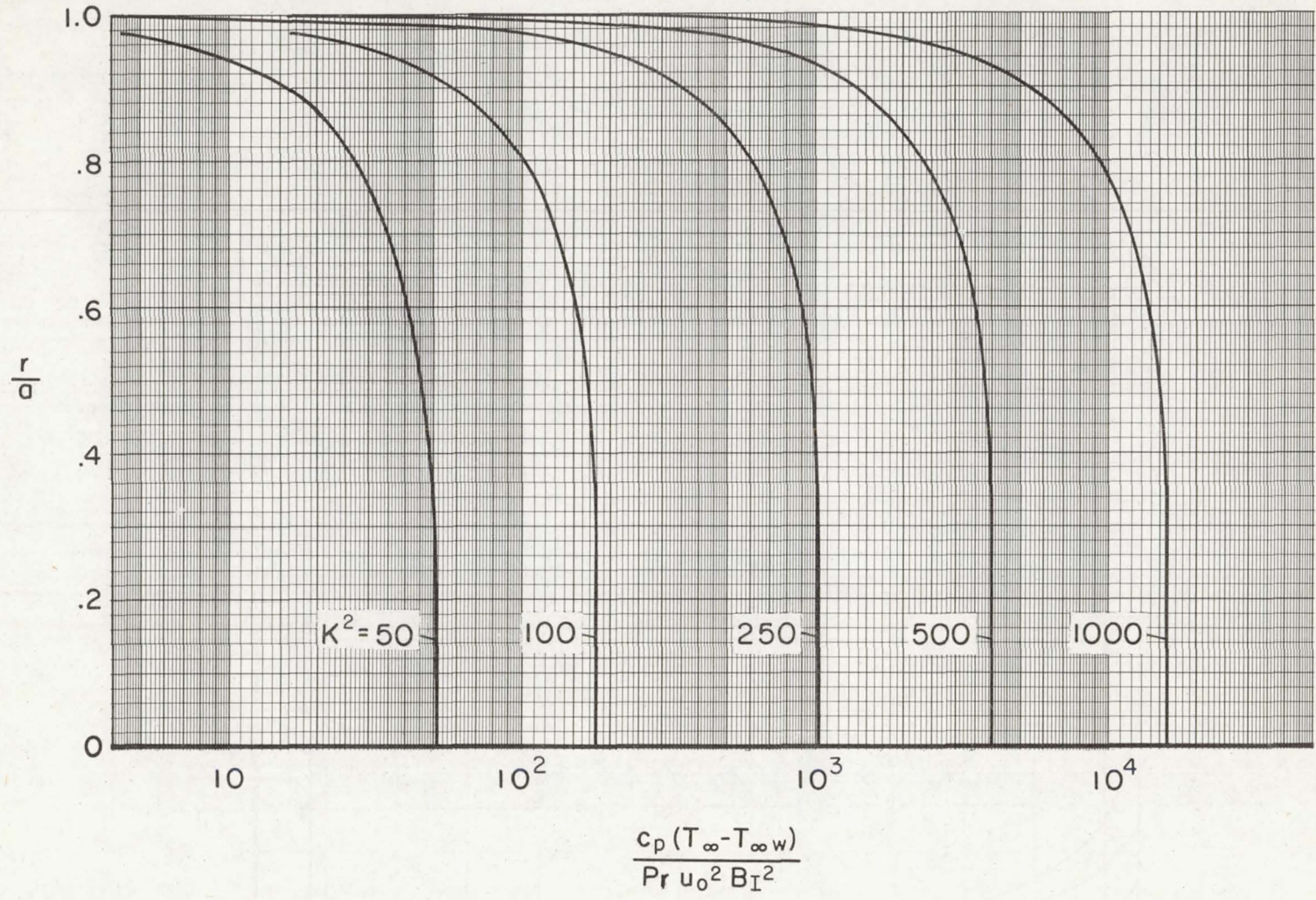
$$\frac{c_p (T_\infty - T_{\infty w})}{Pr\, u_o^2\, B_I^2}$$

(a) Case I.

Figure 5.- Temperature in fully developed flow.
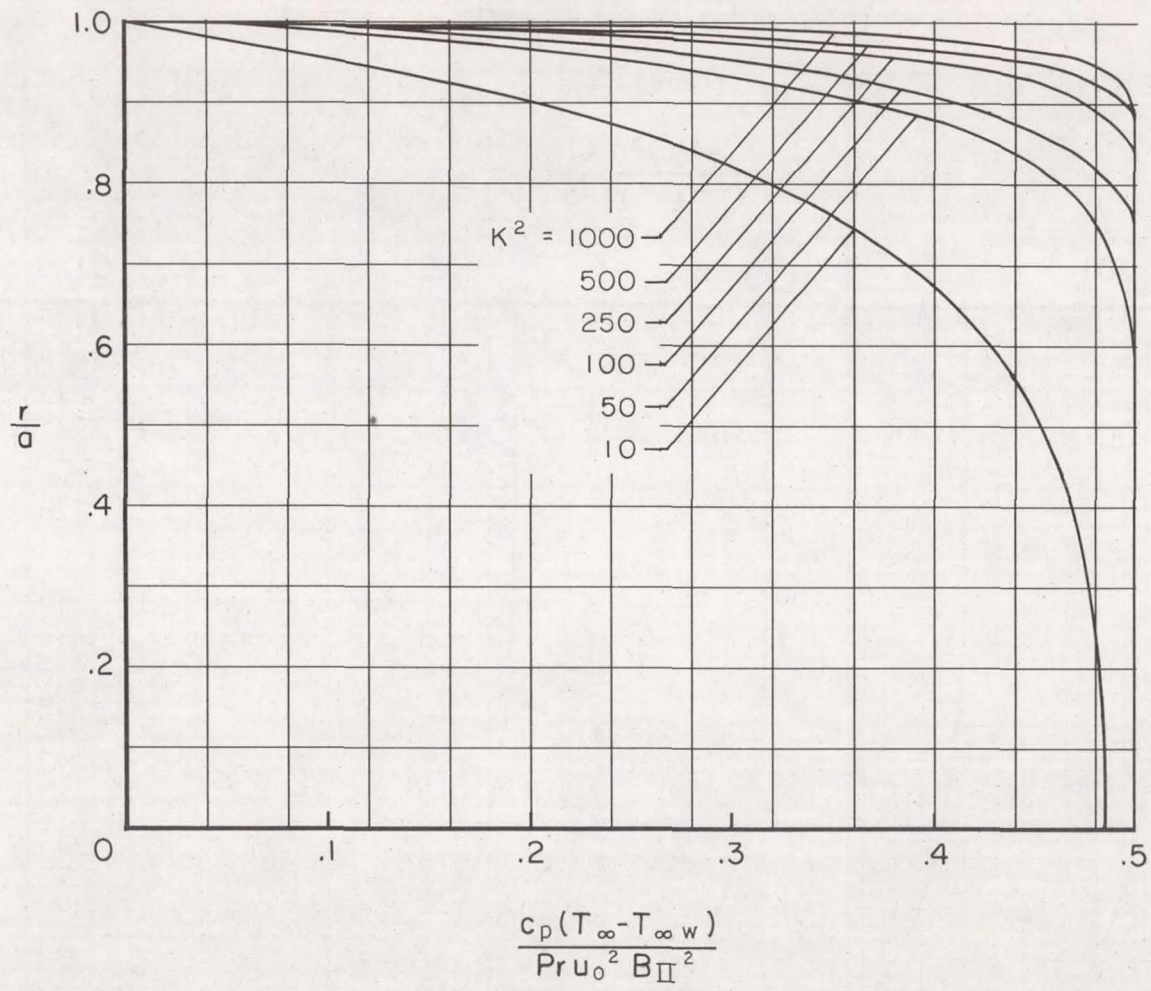
(b) Case II.

Figure 5.- Concluded.
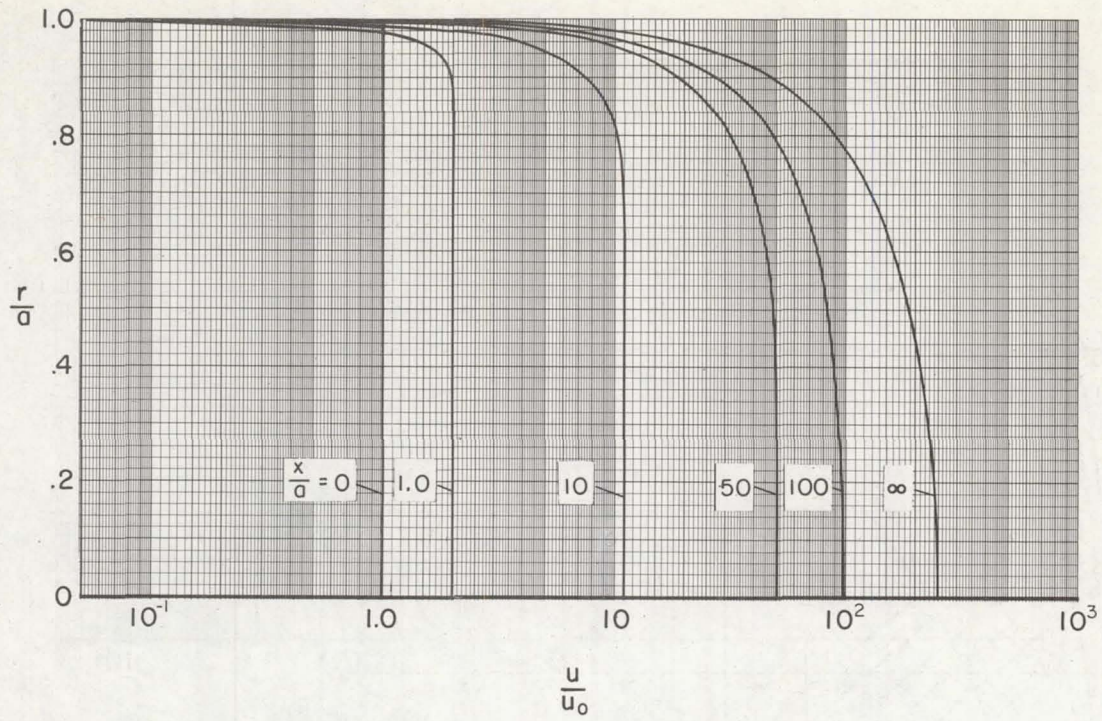
(a) $N_O = 1000$, $K^2 = 1000$, $B_I = 1.0$.
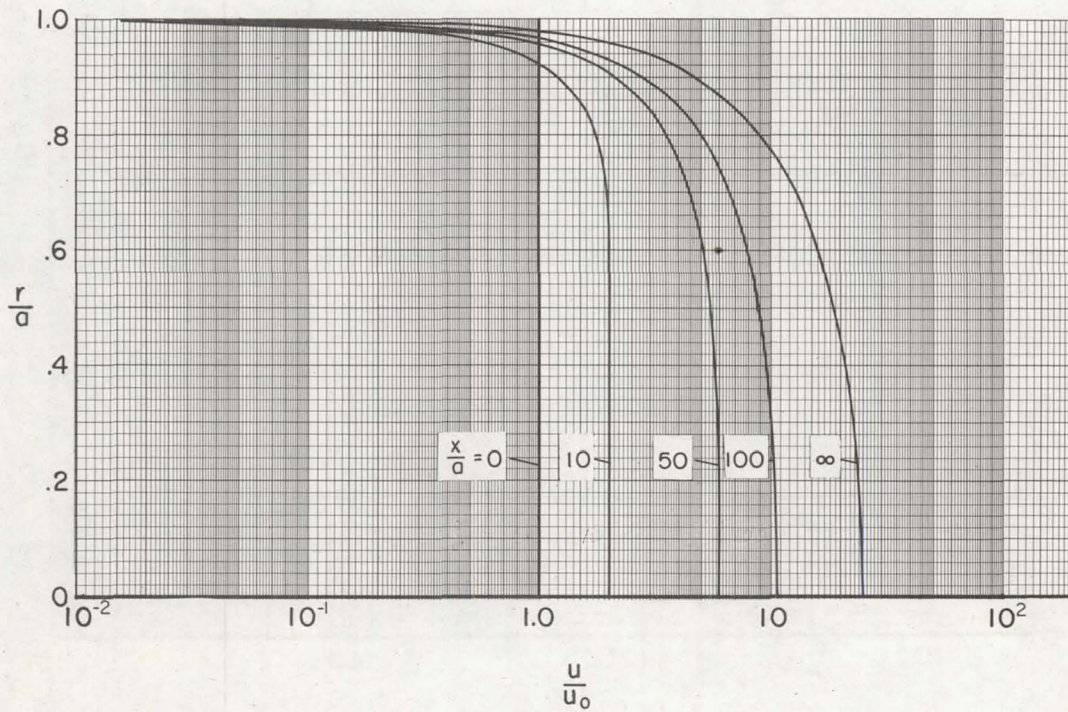
(b) $N_O = 1000$, $K^2 = 100$, $B_I = 1.0$.

Figure 6.- Examples of development of flow from uniform profile; case I.
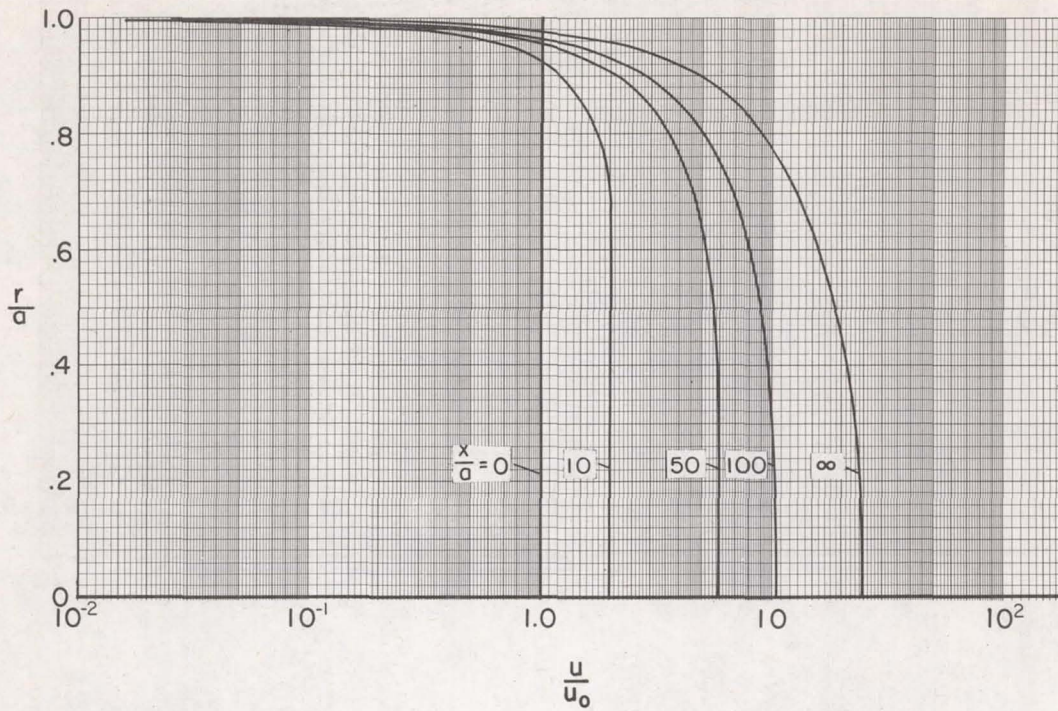
(c) $N_O = 1000$, $K^2 = 1000$, $B_I = 0.1$.
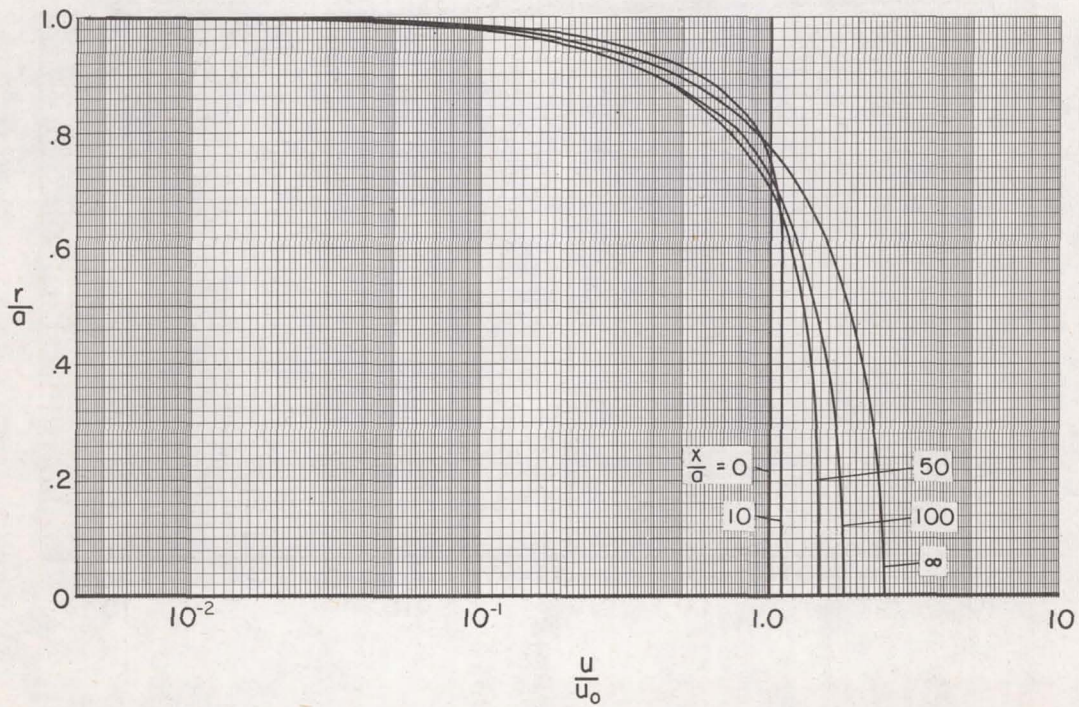
(d) $N_O = 1000$, $K^2 = 100$, $B_I = 0.1$.
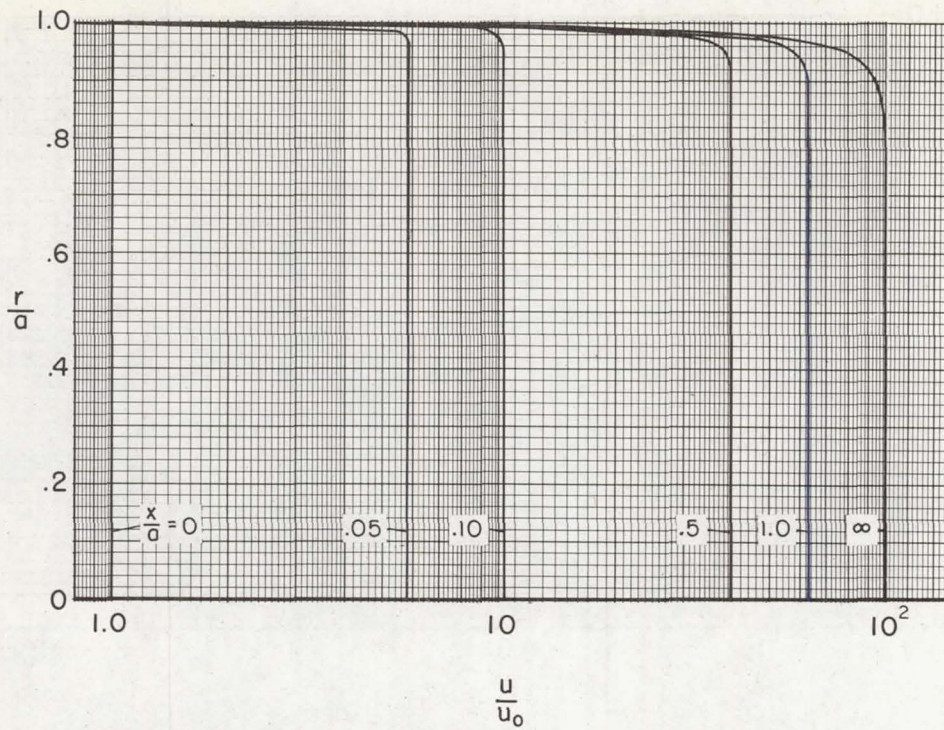
Figure 6.- Concluded

(a) $N_O = 1000$, $K^2 = 1000$, $B_{II} = 100$.
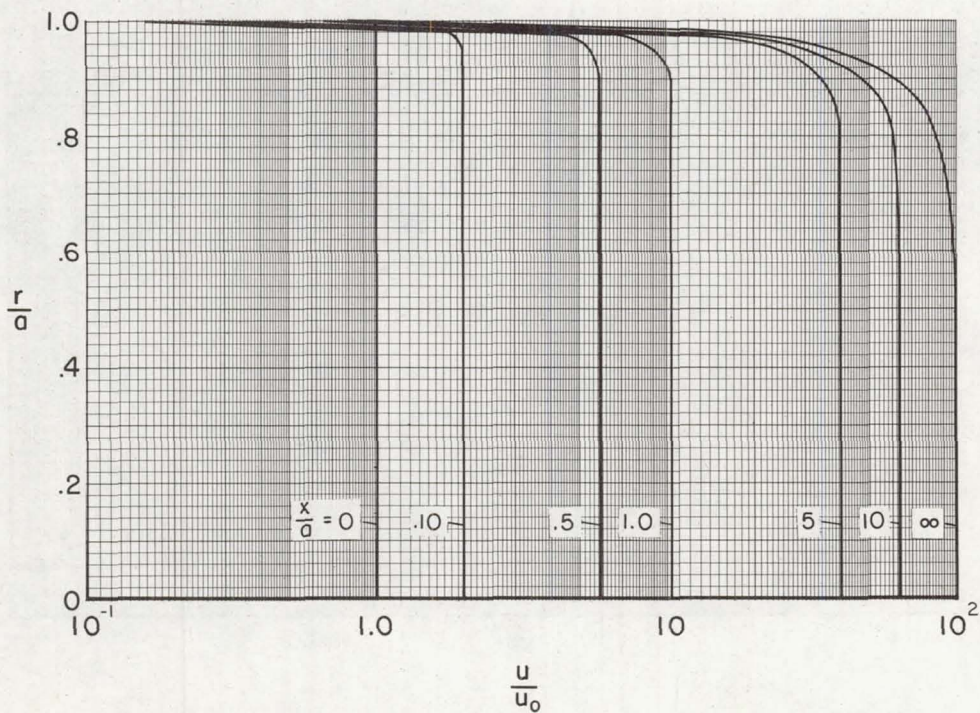
(b) $N_O = 1000$, $K^2 = 100$, $B_{II} = 100$.

Figure 7.- Examples of development of flow from uniform profile; case II.
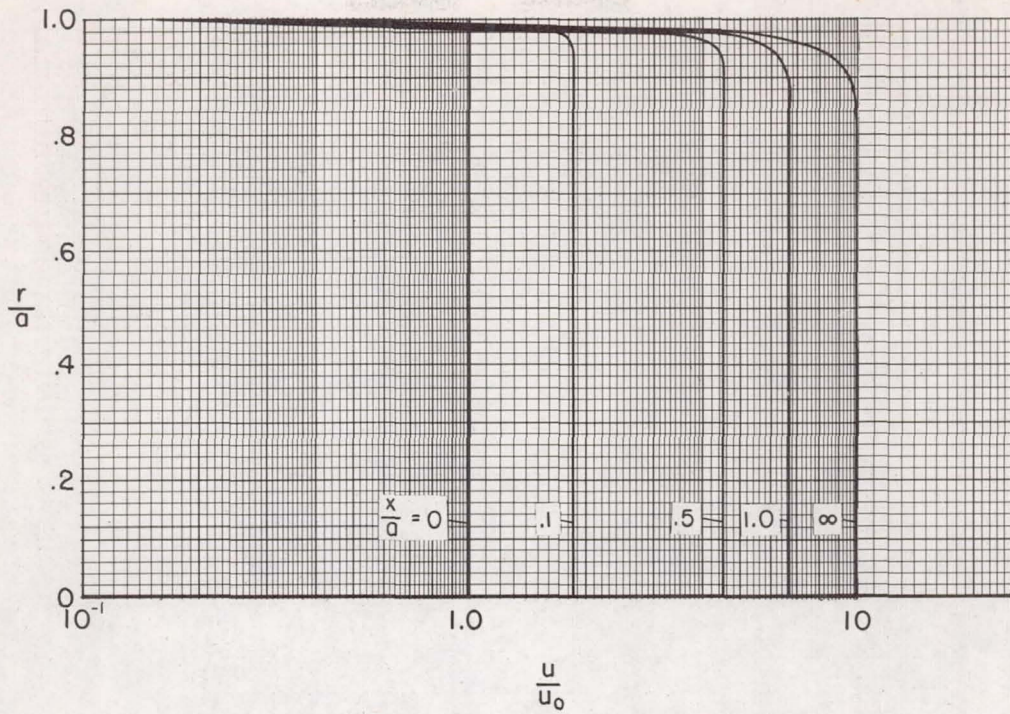
(c) $N_O = 1000$, $K^2 = 1000$, $B_{II} = 10$.
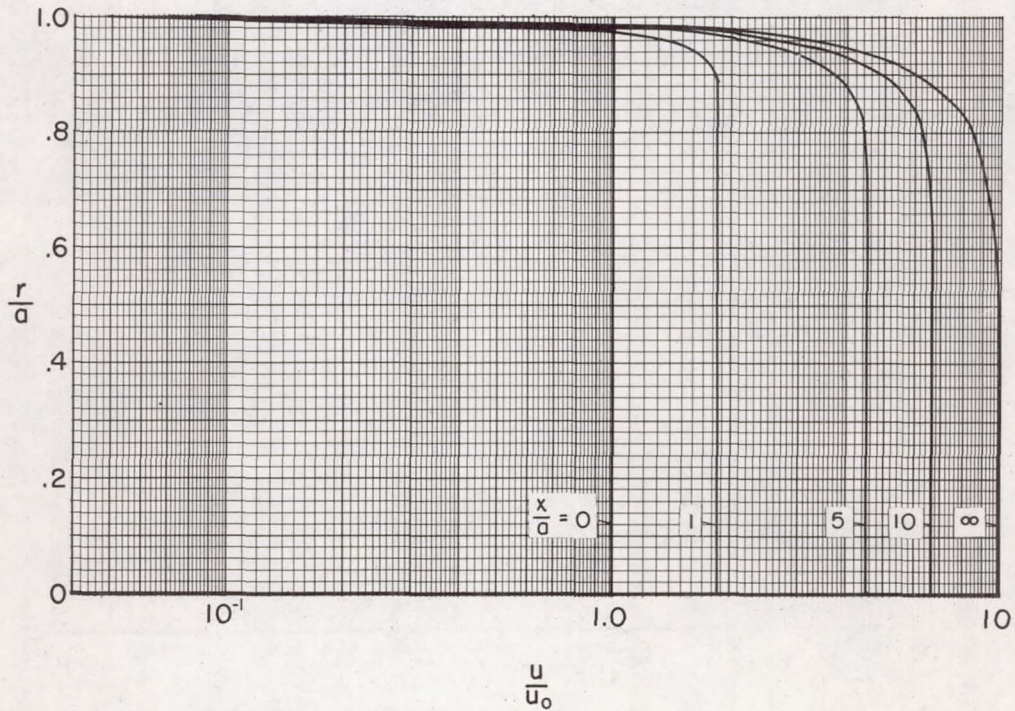
(d) $N_O = 1000$, $K^2 = 100$, $B_{II} = 10$.

Figure 7.- Concluded.
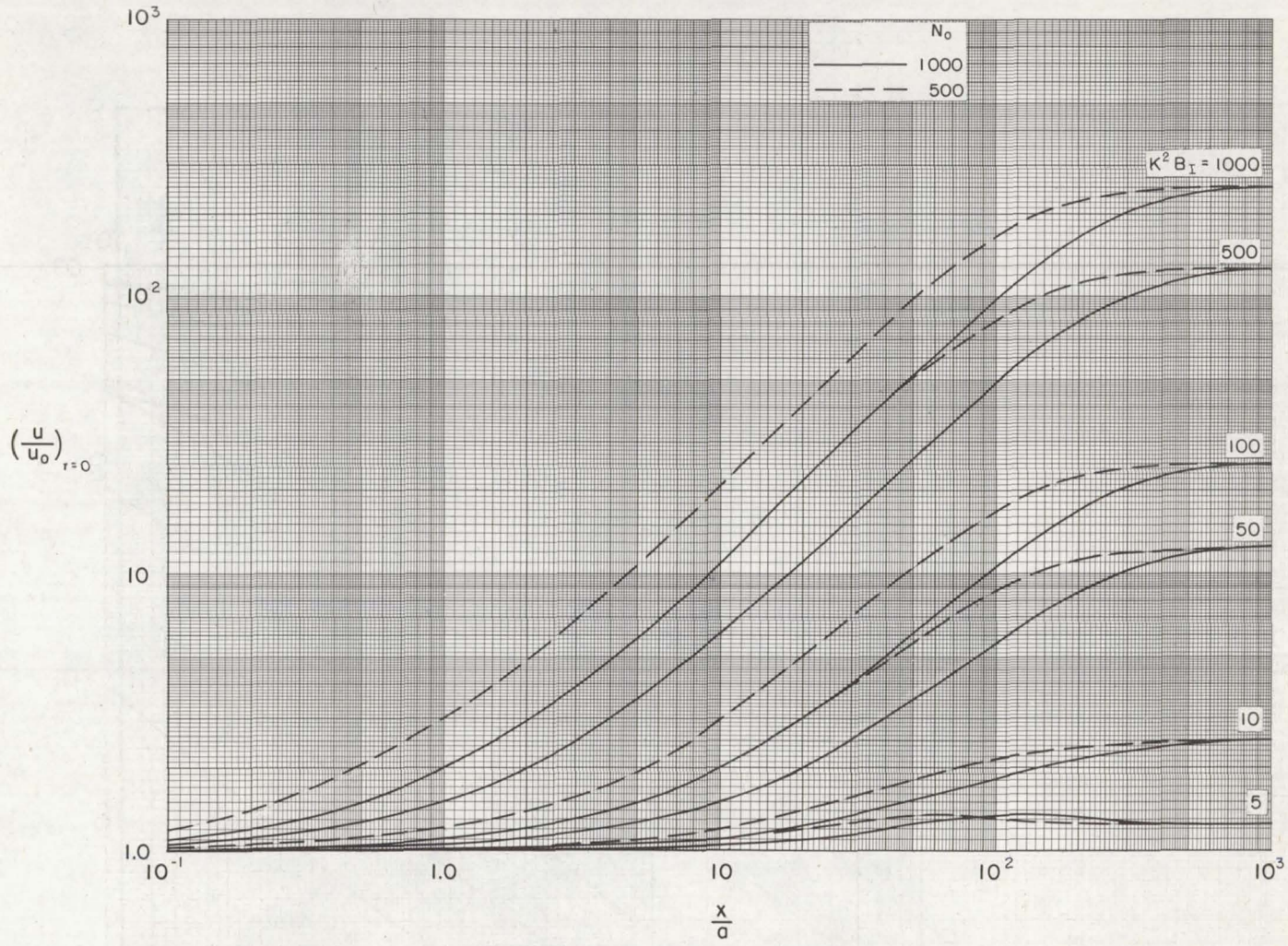
(a) Case I.

Figure 8.- Center-line velocity in accelerating flow relative to inlet velocity.
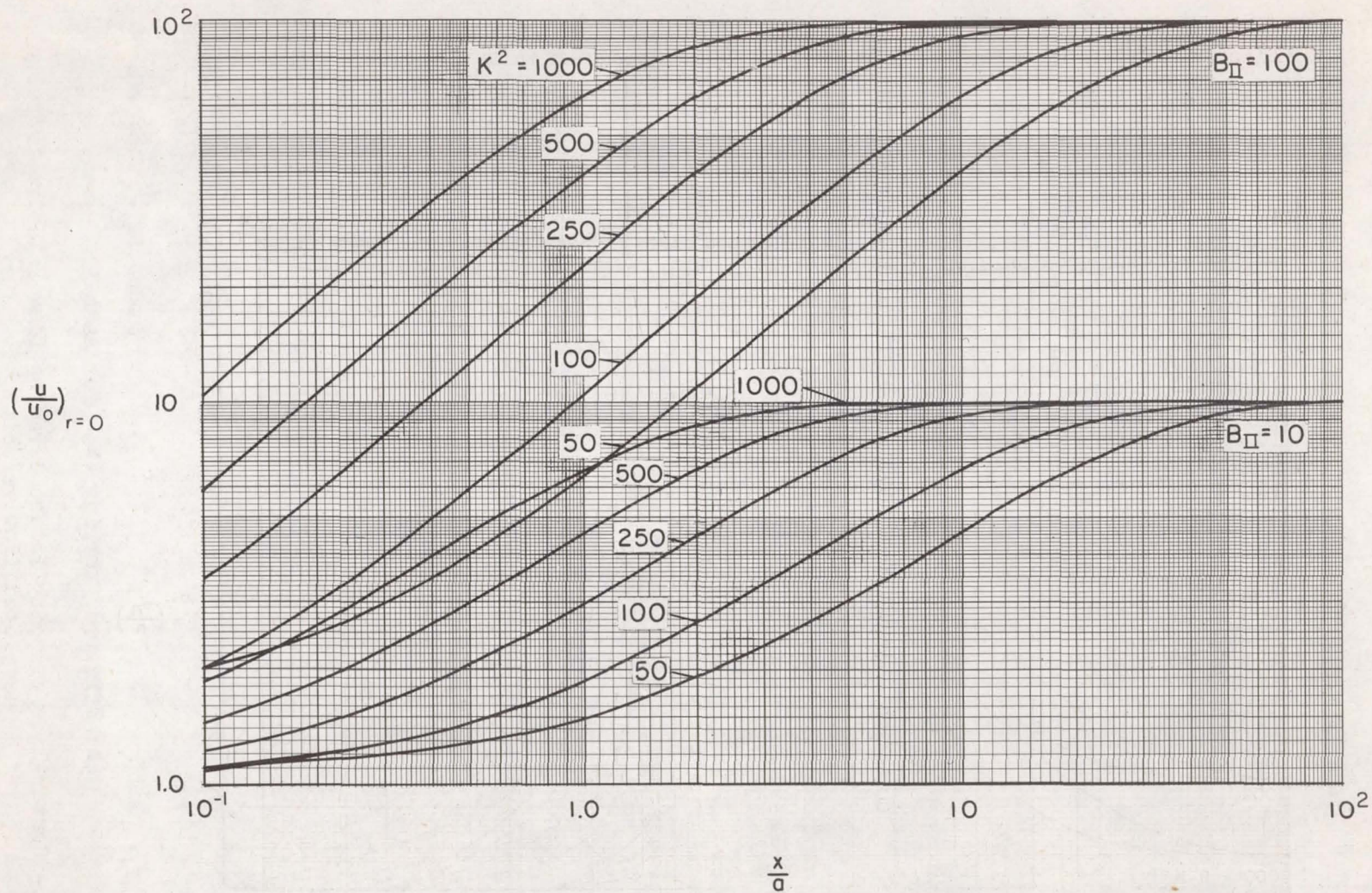
(b) Case II with $N_O = 1000$.

Figure 8.- Concluded.
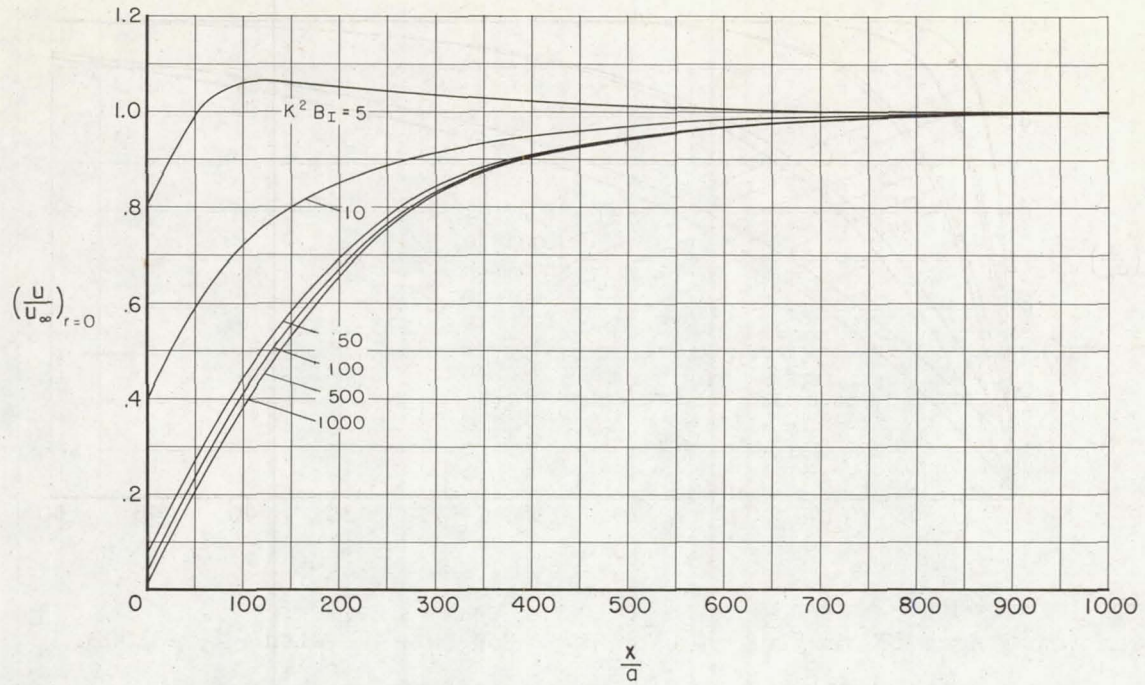
(a) Effect of varying K^2 and B_I for case I with $N_O = 1000$.
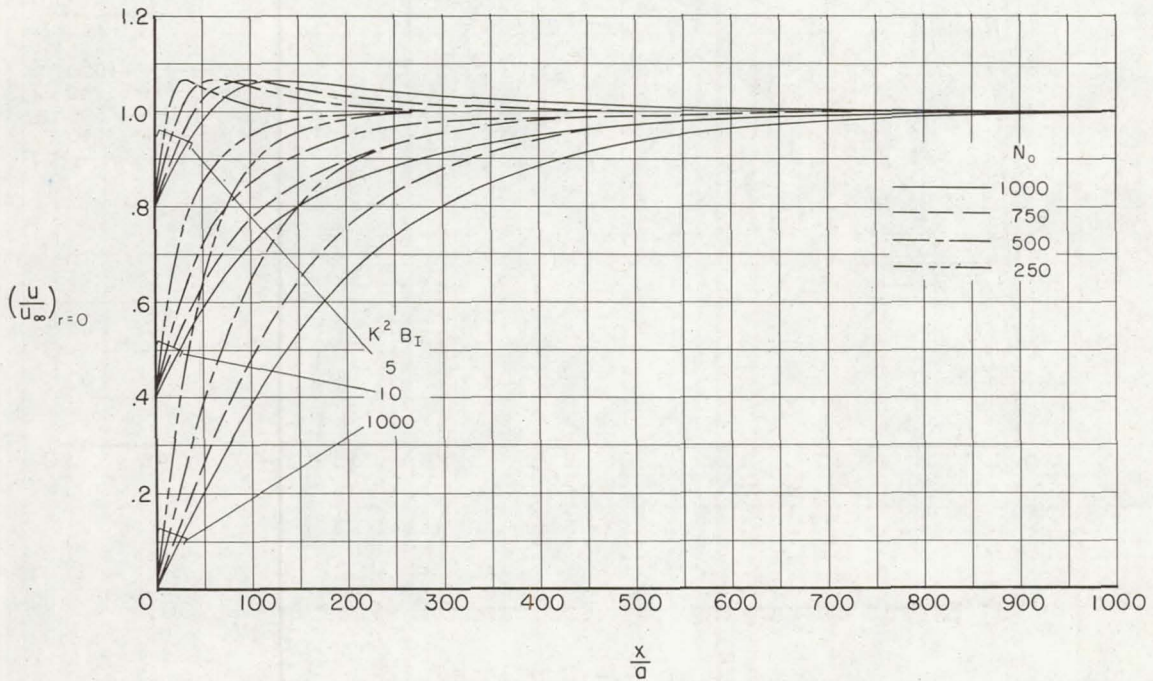
(b) Effect of varying N_O for case I.

Figure 9.- Center-line velocity in accelerating flow relative to fully developed flow velocity.
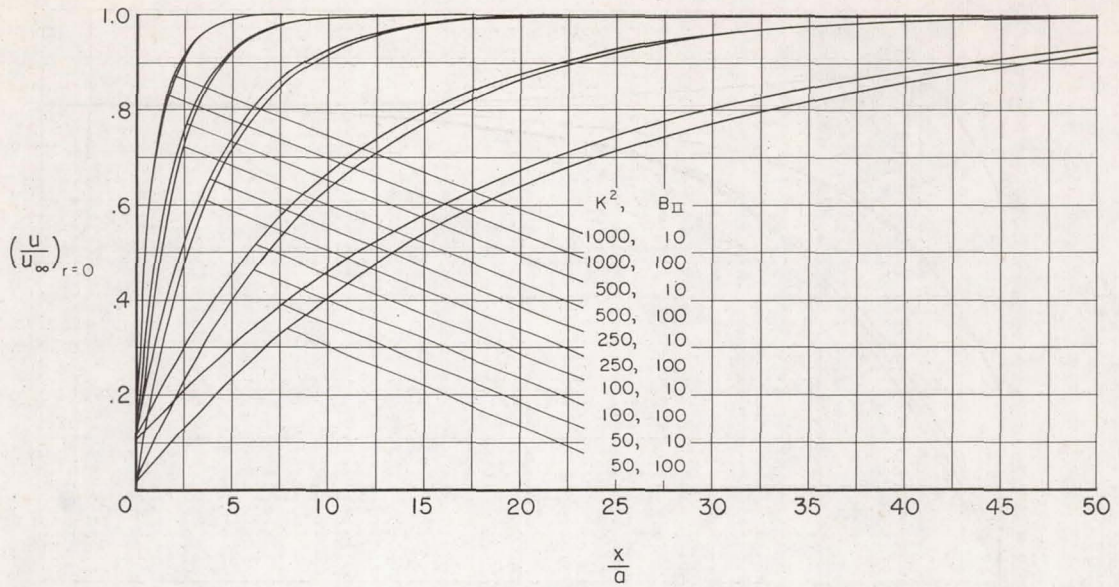
(c) Effect of varying K^2 and B_{II} for case II with $N_O = 1000$.
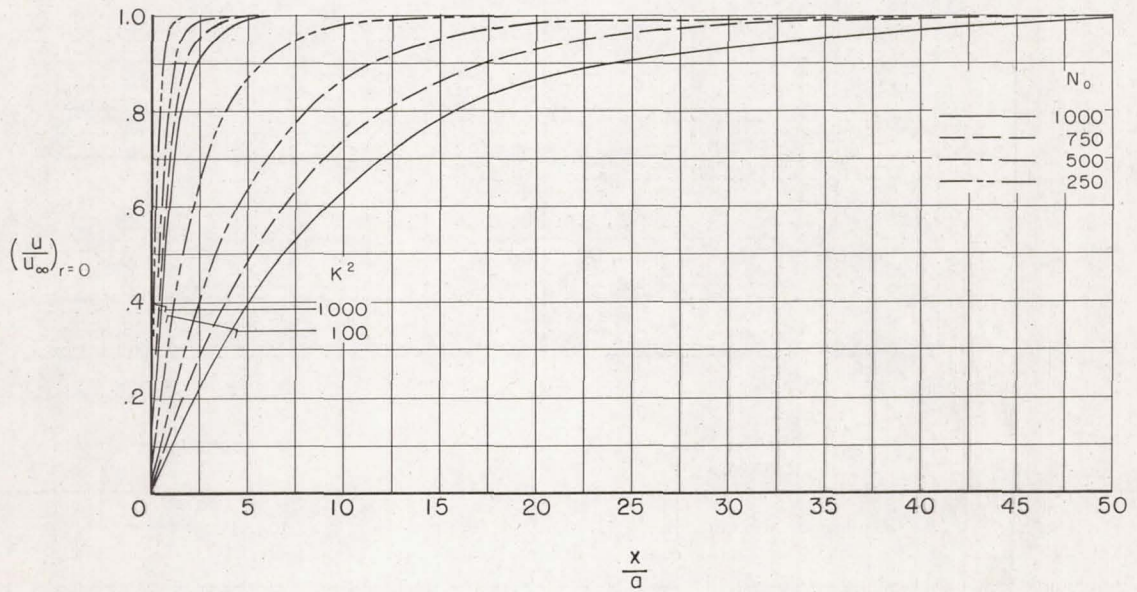
(d) Effect of varying N_O for case II with $B_{II} = 100$.

Figure 9.- Concluded.
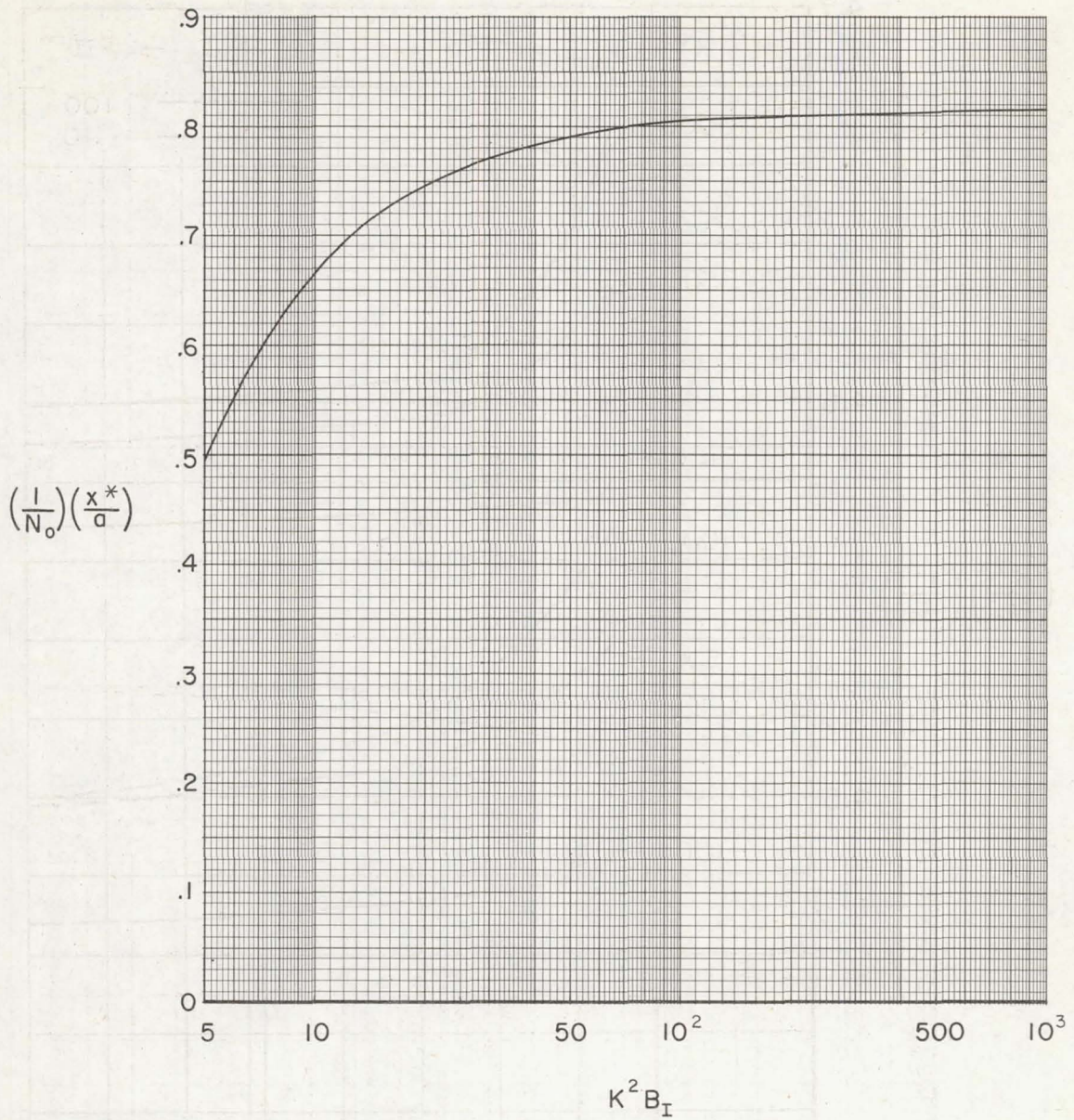
(a) Case I with N_O in the range 250 to 1000.

Figure 10.- Pipe length required to achieve velocity within 1 percent of fully developed flow velocity.

A
3
9
6
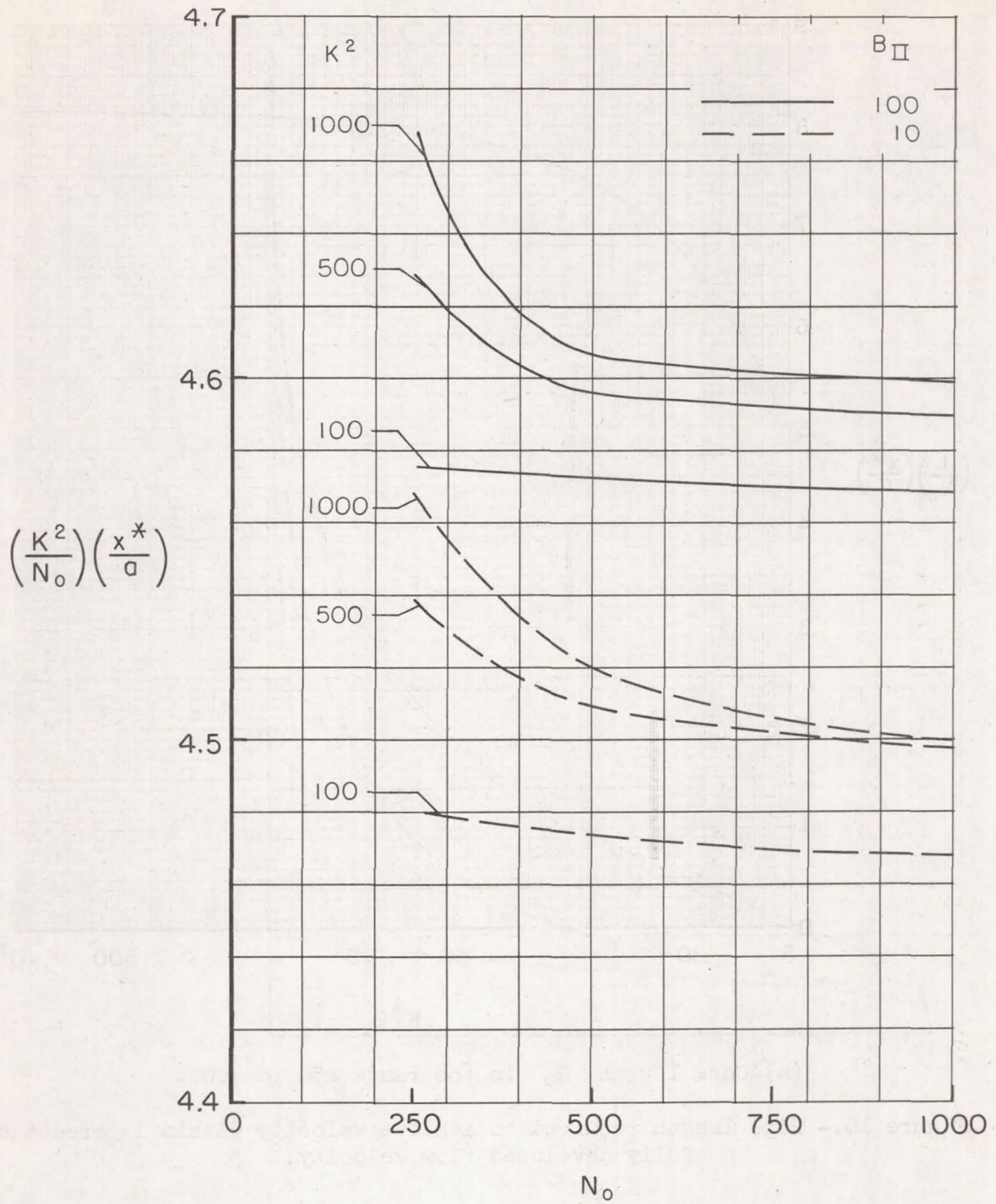
(b) Case II.

Figure 10.- Concluded.
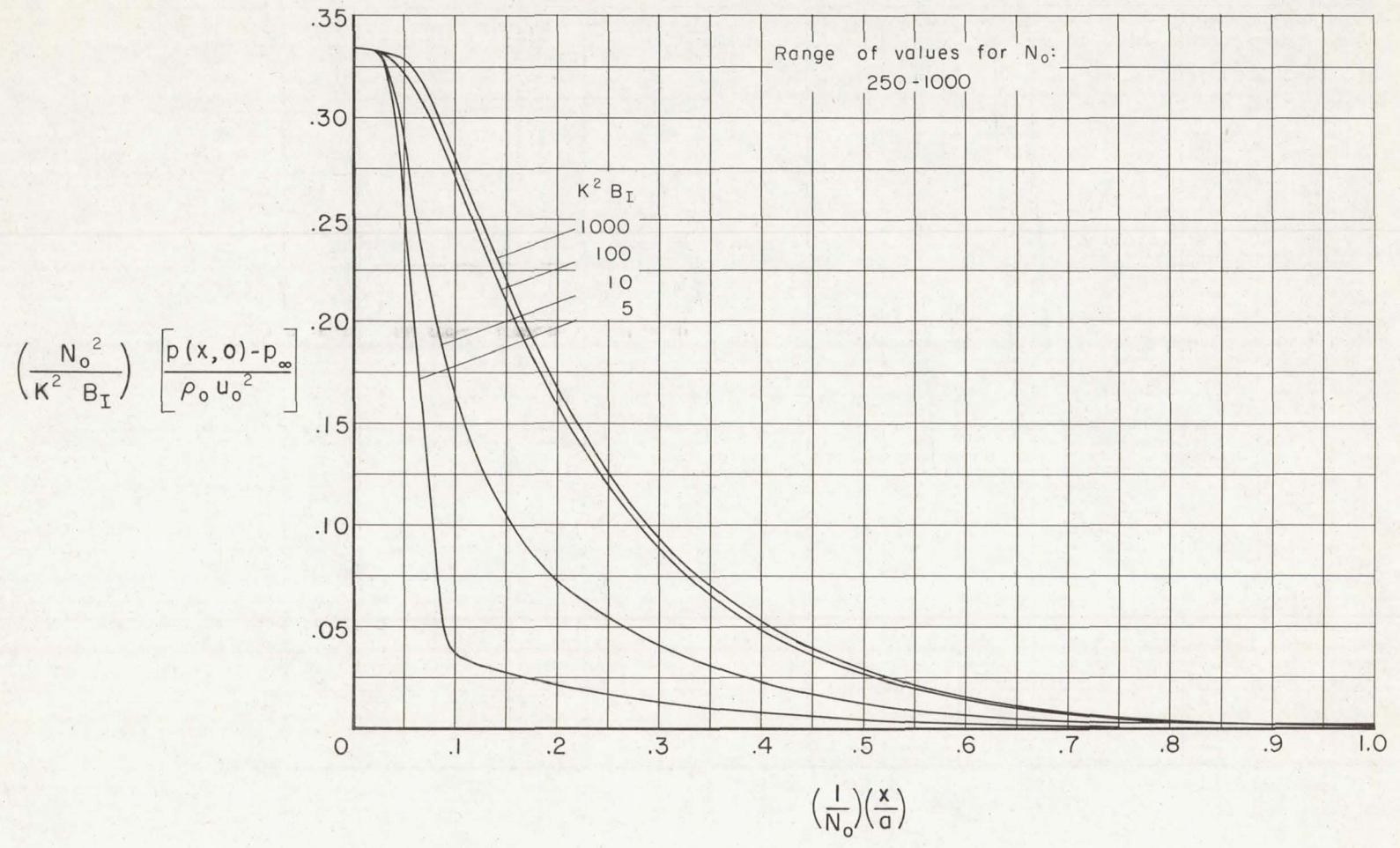
Figure 11.- Center-line pressure in accelerating flow.

(a) Case I.

$$\left(\frac{N_o{}^2}{K^2\, B_I}\right)\,\left[\frac{p\,(x,o)-p_\infty}{\rho_o\, u_o{}^2}\right]$$

$$\left(\frac{1}{N_o}\right)\left(\frac{x}{a}\right)$$

Range of values for N_o:
250-1000

$K^2\, B_I$
1000
100
10
5

$$\left[\frac{N_o^2}{K^2(B_\Pi-1)}\right]\left[\frac{p(x,o)-p_\infty}{\rho_o u_o^2}\right]$$

Range of values for N_o: 250-1000

K^2 50-1000

B_Π 2-100

$$\left(\frac{K^2}{N_o}\right)\left(\frac{x}{a}\right)$$
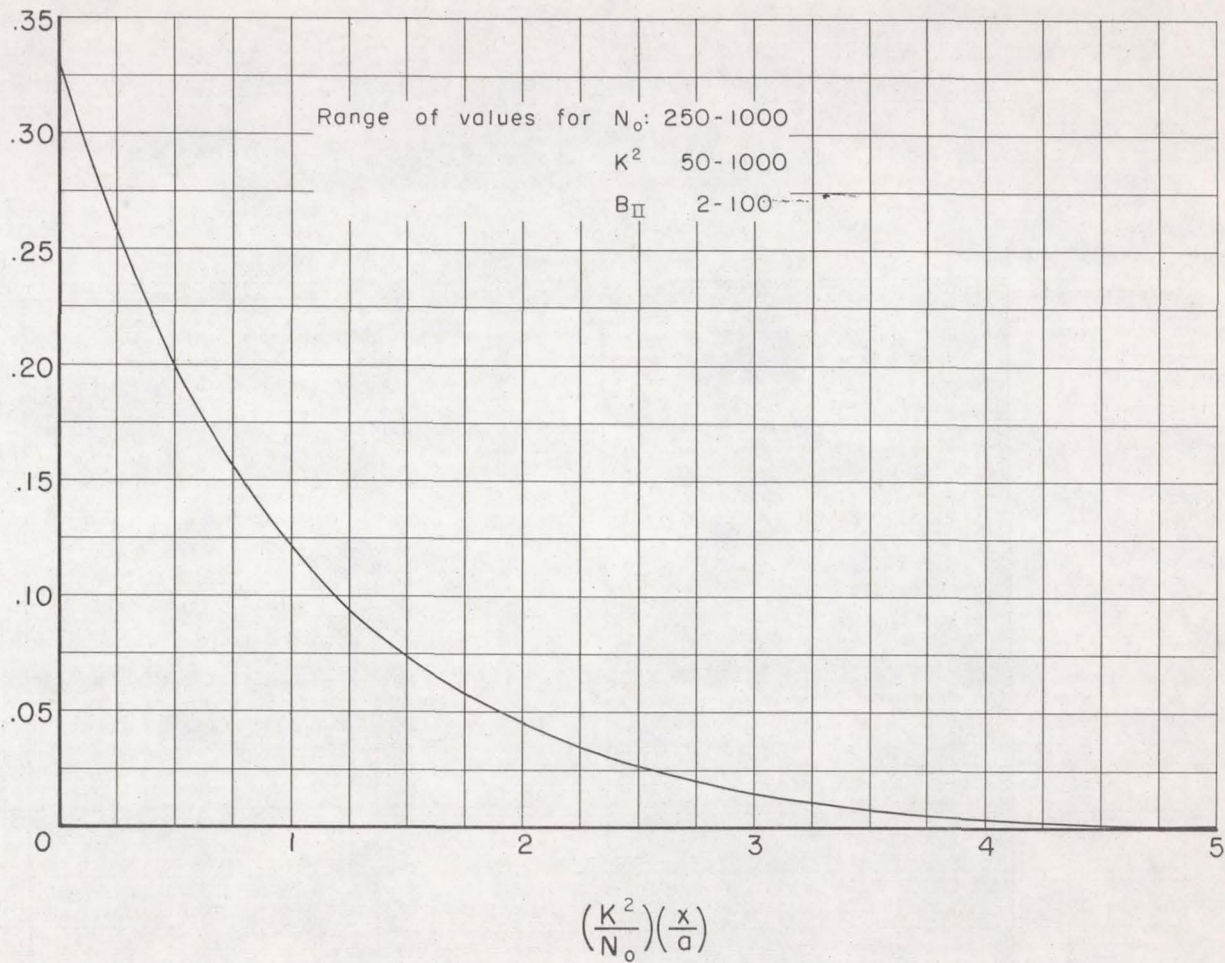
(b) Case II.

Figure 11.- Concluded.
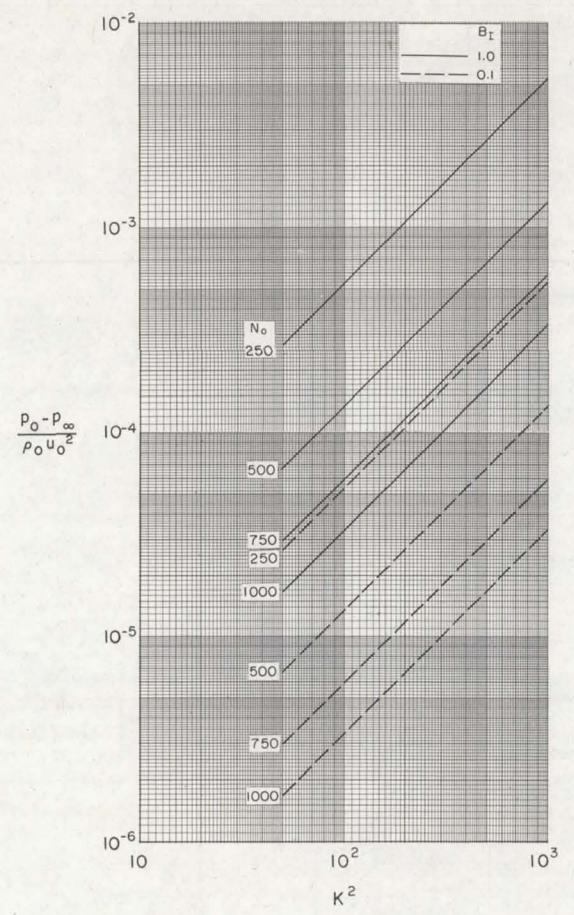
(a) Case I.
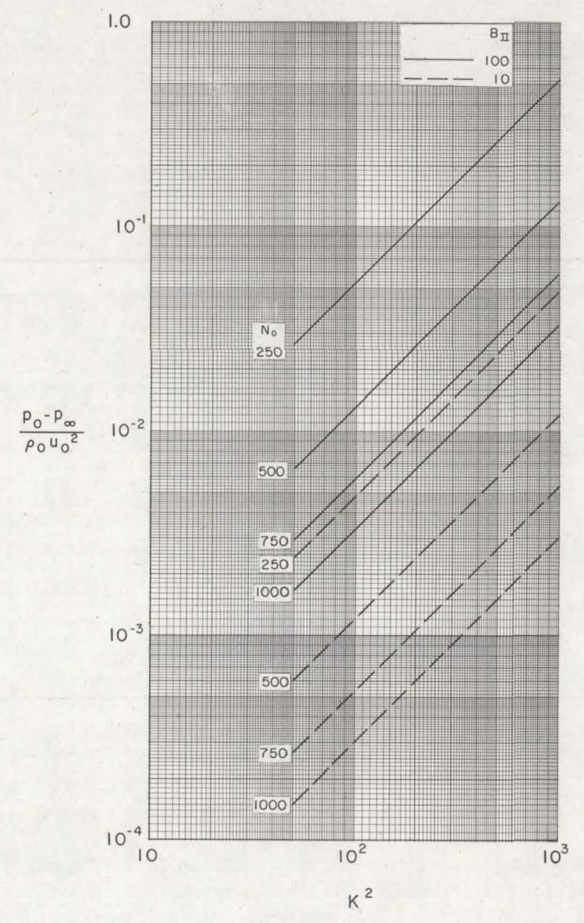
(b) Case II.

Figure 12.- Inlet to fully developed flow pressure difference.
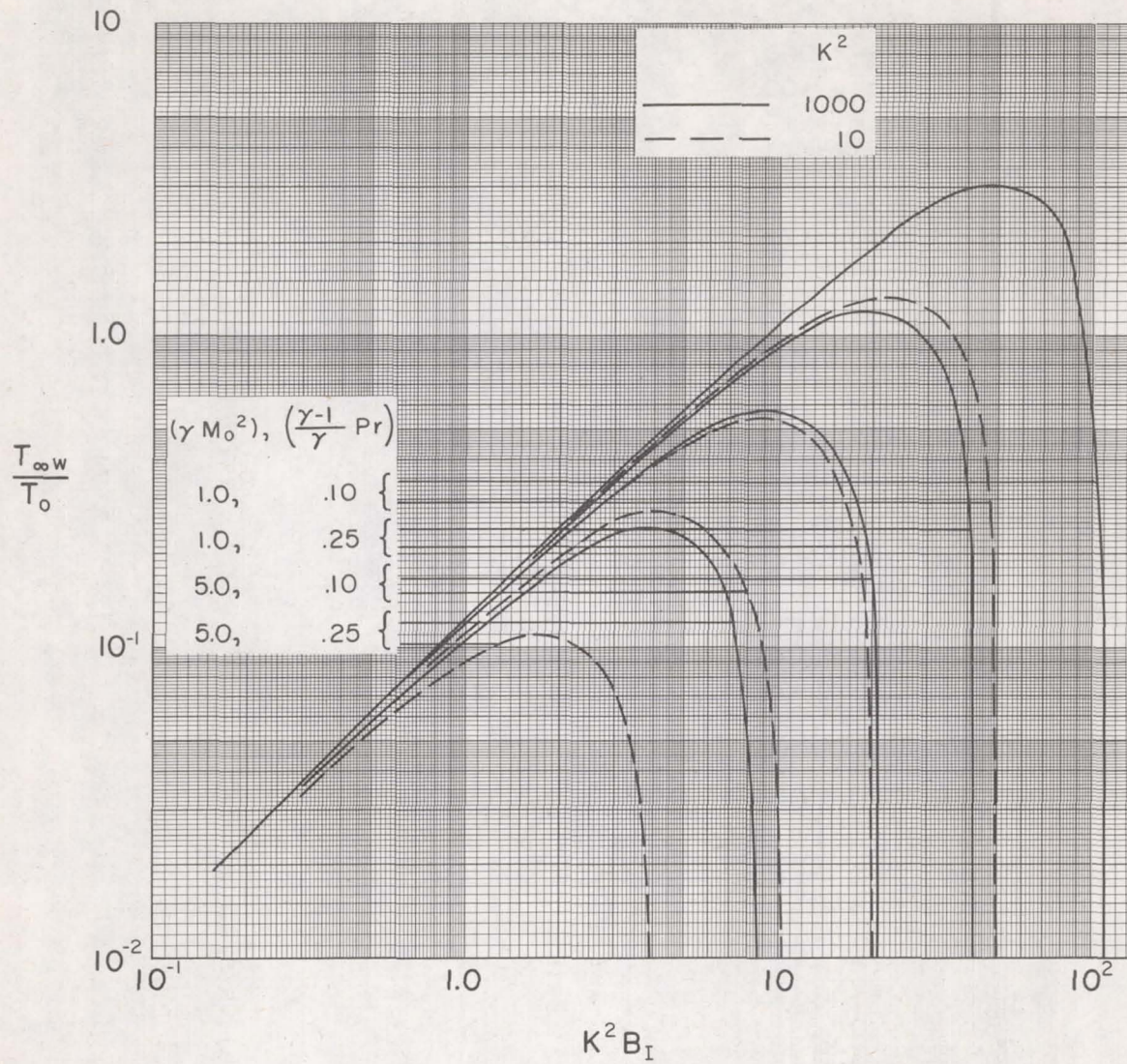
(a) Case I (J_y = constant).

Figure 13.- Relationships among parameters to satisfy over-all continuity (N_O = 1000).
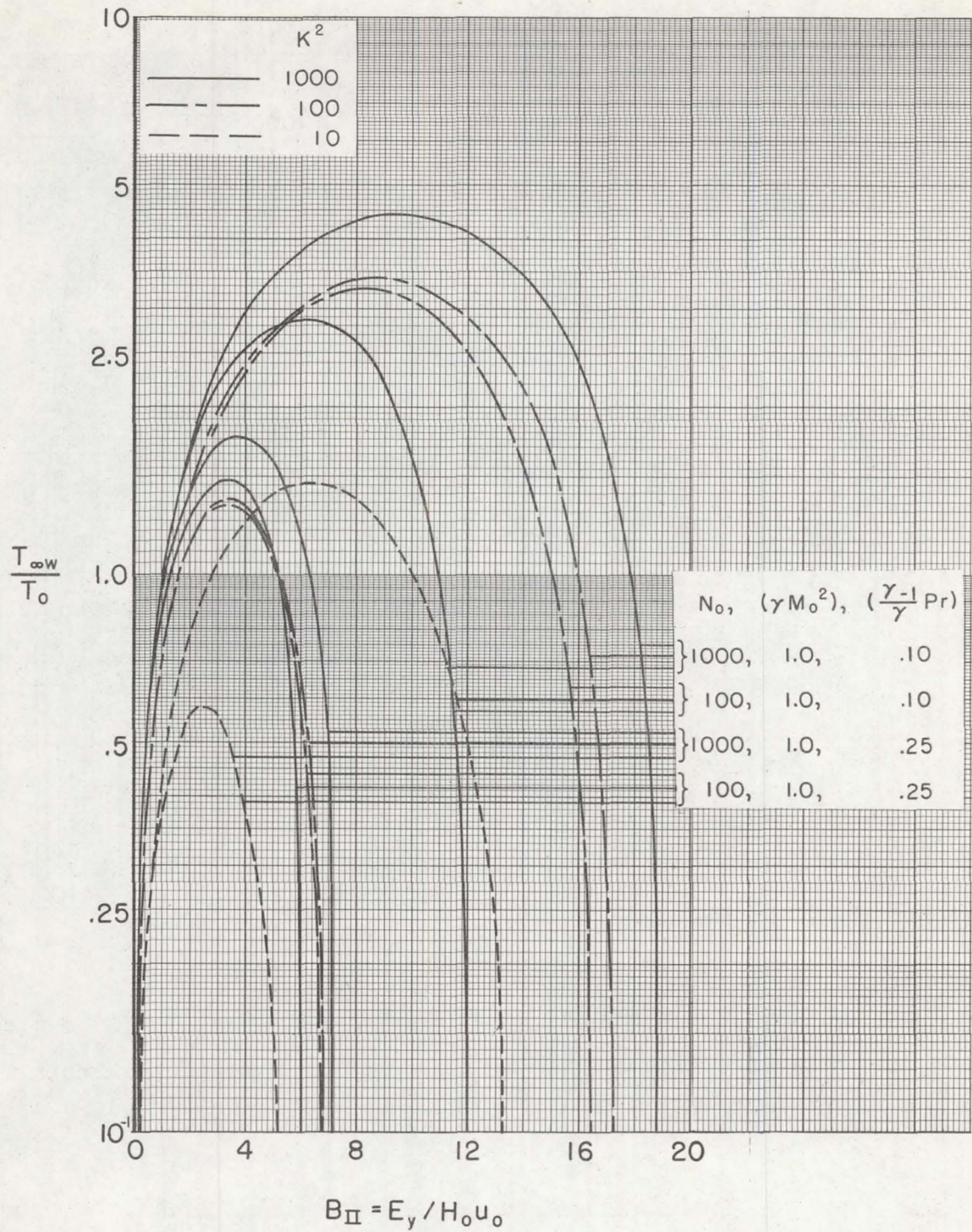
(b) Case II (E_y = constant).

Figure 13.- Concluded.

A
3
9
6
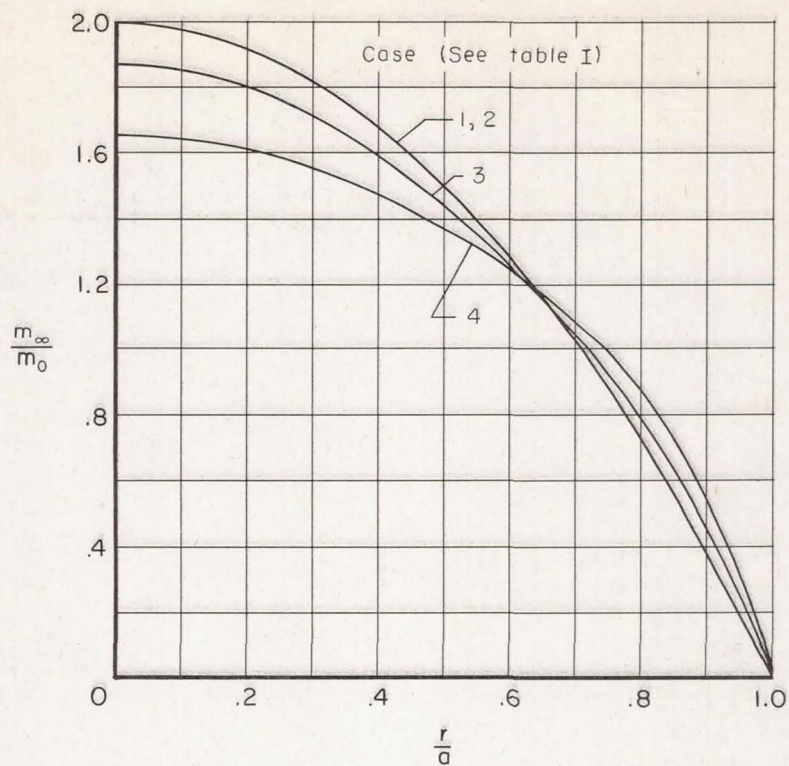
(a) Case I $(J_y = \text{constant})$.
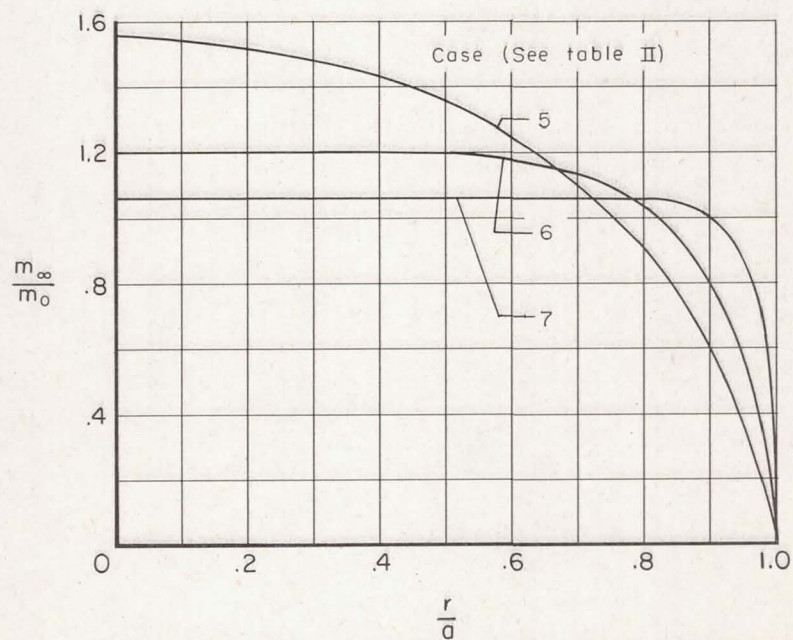
(b) Case II $(E_y = \text{constant})$.

Figure 14.- Mass flow comparison.